NATIONAL ADVISORY COMMITTEE FOR AERONAUTICS

# WARTIME REPORT

ORIGINALLY ISSUED

November 1945 as
Advance Restricted Report E5128 - E - 13

## PRELIMINARY INVESTIGATION OF DEEP INDUCERS AS SEPARATE SUPERCHARGER COMPONENTS

By William K. Ritter and Irving A. Johnsen

Aircraft Engine Research Laboratory
Cleveland, Ohio

NACA

WASHINGTON

NACA ARR No. E5I28

NATIONAL ADVISORY COMMITTEE FOR AERONAUTICS

ADVANCE RESTRICTED REPORT

# PRELIMINARY INVESTIGATION OF DEEP INDUCERS AS SEPARATE SUPERCHARGER COMPONENTS

By William K. Ritter and Irving A. Johnsen

## SUMMARY

A family of three single-stage deep inducers was designed to impart solid-body, or wheel, rotation to the entering air at constant rates along the axial depth of the inducers. The cast inducers tested were 4-inch axial depth with 24 blades, 4-inch depth with 12 blades, and 2-inch depth with 24 blades. An inducer (bent-bucket) section cut from a conventional production impeller was tested in the same test rig for comparison. Tests of all models as separate supercharger components determined the efficiencies as compressors and the angular velocities imparted to the air. The 4-inch, 24-blade inducer was tested with unfinished and with elliptically rounded entrance edges. The tests of cast inducers were limited to tip speeds equivalent to 800 and 1000 feet per second of the impellers for which the inducers were designed because of strength limitations of the castings. Air flow through the inducers was controlled independently of inducer speed.

The 4-inch, 24-blade inducer with rounded entrance edges produced a near approach to wheel rotation of the discharged air and had a peak adiabatic efficiency of 80 percent, 7 points above that obtained with unfinished entrance edges, at a flow quantity near the design load coefficient. Rotational-velocity characteristics were independent of speed within the range of the tests and the adiabatic efficiencies of each inducer showed a marked similarity over the speed range. The efficiency of the conventional inducer was low in the operating range of the impeller of which it was a part and continuously increased with increasing load coefficient.

## INTRODUCTION

Compression in a centrifugal supercharger is accomplished by increasing the moment of momentum of the air by means of an increase in angular velocity and in the radius of rotation of the air as it flows through the impeller. The supercharger component that imparts the angular velocity of the impeller to the entering air has been designated an inducer by the NACA Subcommittee on Supercharger Compressors. The inducer may be designed as an integral part of the impeller or as a separate component to impart rotational velocity to the air before it enters the impeller proper.

The inducer function of imparting angular velocity to the entering air may cause large direct losses, and disturbances of flow in the inducer may affect the functioning of all other supercharger components. The inducer is believed to be one of the least efficient components of conventional centrifugal superchargers, but little information directly relating to the functioning of inducers is available. The efficiency of a DVL supercharger was increased approximately 8 points by the use of a separately added impeller (inducer) according to the tests reported in reference 1. This improvement was obtained by tests of several inducers but no comparative results for the several inducers are presented. The development of inducers having low losses and properly matched to their impellers should result in direct improvement in supercharger performance. Many problems of supercharger research, including the shape of impeller passages, cannot be properly investigated until efficient inducers having large flow capacity are designed.

As part of a program to investigate the requirements and the design criteria of inducers and the relation between inducers and impellers, a family of single-stage inducers was designed and constructed to permit the testing of each of the inducers with each of a series of impellers. The present report covers preliminary tests of three of the family of single-stage deep inducers and of an inducer section cut from a conventional impeller. The inducers were tested as separate supercharger components and, in the absence of an adequate theory of inducer functioning, ratings were made on the bases of compressor efficiency and approach to solid-body rotation of the discharge air

The tests were made at the NACA laboratory at Langley Field from April to June 1943. The results of the tests were given limited publication among the aircraft-engine industry. Inducers based on these designs have been applied to some military engine superchargers and excellent results reported.

## CONSTANT-ANGULAR-ACCELERATION INDUCERS

### Design

A family of three single-stage deep inducers was designed for lower blade loading and more gradual angular acceleration than in the bent-bucket entrances of conventional centrifugal impellers. Two entrance-edge forms were used with one of the three designs. The short-radius circular-arc bending used in conventional impeller-inducer sections cannot be proportionally continued into the hub of the initially straight blades nor can the blade be set at the optimum angle to the air stream along the entire leading edge. These short-radius circular-arc curvatures impose a very high initial tangential acceleration on the entering air and a decreasing tangential acceleration on the air passing axially through the inducer. This high loading at the leading edge has a precedent in some airfoil designs and the decreasing loading through the inducer might be expected to inhibit separation; but the high loadings of the conventional bent-bucket designs are beyond the expected possibilities for smooth flow.

Because the most gradual air-flow acceleration possible was desired, the single-stage deep inducers were designed for constant angular acceleration over the axial depth. This design basis gives an inducer-blade profile which, developed on a plane, is a parabola. Each of the inducers was designed to impart wheel rotation to the air at the design operating conditions and each has the same entrance angle. The acceleration is thus inversely proportional to the axial depth and the blade loading depends on the axial depth and the number of blades. This design is based on the simplifying assumptions that (1) the axial velocity of the air remains constant and uniform — that is, compressibility and wall effects are excluded – and (2) that the air follows the blade surfaces.

Inducers were designed with axial depths of 4 and 2 inches, a constant hub diameter of 3 inches, and a constant outside diameter of 8 inches. The design conditions for these inducers were an axial inlet velocity of 300 feet per second and a tip speed of 1200 feet per second of the 12-inch-diameter impellers for which the inducers were designed. These design conditions correspond to a load coefficient of 0.24. A blade-inlet angle of attack of $5^{\circ}$ at the root-mean-square diameter was used. The angle of attack is stated with reference to the mean camber line of the blades, using the airfoil convention of signs. Blade center lines are radial and blade thicknesses are proportioned to make the blade elements straight lines. The entrance edges of the blades are rounded to an elliptical profile similar to that of high-speed airfoils. The hub and the outside

diameters were maintained constant in this design in order to adapt the inducers interchangeably to specific impeller designs. The 4-inch, 24-blade inducer with rounded entrance edges is shown in figure 1.

In order to determine the effect of the entrance edge, a 4-inch, 24-blade inducer was also tested with unfinished entrance edges, that is, sharp edged as formed by lathe turning and having a flat surface perpendicular to the axis of the inducer.

On the assumption that rotation was induced by the lift forces of the blades as airfoils, the required lift coefficients were computed. Although the numerical values of the lift coefficients of the inducer blades have doubtful significance, they do permit a comparison with those of the conventional bent-bucket entrances. The required lift coefficients of the inducer blades at design flow conditions are shown in figure 2. The bent-bucket inlet section tested for comparison had a lift coefficient of 3.0, calculated at the root-mean-square diameter for the design flow conditions of the impeller.

The variation in passage area along a mean flow-path line at the root-mean-square diameter for the three deep-inducer designs is shown in figure 3. The passage-area variations in these designs are functions of the axial depth, the blade angle, and the number of blades. The uniform hub diameter and outside diameter did not permit passage-area control by changing passage boundaries.

## Construction

The test inducers were aluminum-alloy castings made at the NACA Langley Field laboratory. Casting was chosen as the quickest method of producing a sufficient number of inducers for these particular tests. The only objectives were good dimensional accuracy and sufficient strength for tests at reasonable tip speeds. A technique using cast-aluminum core boxes in which the dry-sand cores were formed and baked proved satisfactory. Considerable experimentation in core assembly and pouring technique was required.

For comparative tests a production-type inducer was obtained by removing the inlet section from a conventional impeller, which had bent inlet buckets with a circular-arc profile bent to an angle of 36° with the front face at the 8-inch diameter. The curvature of the bending was not proportional to the radius and did not extend to the hub. The section was cut to give an axial depth of $1\frac{5}{16}$ inches, which made the axial depth of the inducer approximately

1/16 inch more than the maximum depth of bending at the 8-inch diameter. This 22-blade inducer was reworked to a constant outside diameter of 8.0 inches and a constant hub diameter of 3.5 inches to adapt it to the inducer test rig.

A design comparison of the cast deep inducers and the inducer cut from the impeller is as follows:

| Type | Axial depth (in.) | Number of blades | Blade entrance edge | Hub diameter (in.) | Blade form | Blade lift coefficient (at rms diam.) |
|---|---|---|---|---|---|---|
| Cast deep inducers | 4 | 24 | Unfinished | 3 | Constant tangential accelera-tion | 0.43 |
| | 4 | 24 | Rounded | 3 | | .43 |
| | 4 | 12 | ---do----- | 3 | | .86 |
| | 2 | 24 | ---do----- | 3 | | .86 |
| Inducer from conventional impeller | $1\frac{5}{16}$ | 22 | Production finish | 3.5 | Bent bucket | 3.0 |

## APPARATUS

The inducer test rig. - A photograph of the test installation, an adaptation of the variable-component supercharger test rig described in reference 2, is shown in figure 4. The inducer was driven by an electric dynamometer through a step-up gear box. A schematic layout showing the mounting of the inducer and instruments is given in figure 5. A separately driven exhauster was connected to the collector discharge and a throttle valve was placed in the discharge duct. This arrangement permitted independent regulation of air flow and inducer speed.

Instrumentation. - Measurements of temperatures and pressures were made in accordance with the recommendations of references 2 and 3 where applicable. The instrument locations are shown in figure 5. Temperatures were measured with calibrated iron-constantan thermocouples, which had a common cold junction in melting ice; the potentials were measured by a calibrated potentiometer equipped with an external spotlight galvanometer. Static and total pressures were measured with either tetrabromoethane or mercury manometers according to the magnitudes of the pressures.

The speed of the inducer was maintained at the desired constant value with a speed strip and a 60-cycle stroboscopic light. Frequent checks were made with a revolution counter and a stop watch.

A two-hole cylindrical directional tube was mounted 1/2 inch ahead of the inducer to make radial surveys of the direction of flow into the inducer. Static and total pressures were taken in the inlet pipe 2 diameters ahead of the test section. A series of static taps 0.020 inch in diameter were located in the test-section wall at approximately 1-inch intervals along the inducer axial depth. The state of the air discharged from the inducer was determined by measurements made in a plane 1/2 inch behind the inducer. A two-prong pitot-tube yaw head with a third pitot tube bisecting the angle was used to measure direction of flow and total pressure in the direction of flow at the inducer discharge. (In later tests a two-hole cylindrical directional tube was added to obtain measurements at the wall of the test chamber.) A static tube having a thin disk pierced at the center and a bare thermocouple were used together with the other instruments at the inducer discharge for taking radial surveys.

The weight of air entering the inducer was determined from velocity and static pressures measured by a pitot-static tube located in the inlet pipe 2 diameters ahead of the test section. The tube was located at the point of average velocity determined by calibration tests made over a range of air flows. Constant air flow was maintained by regulating the exhauster speed or by throttling to keep constant pressure on an NACA micromanometer connected to the throat of an uncalibrated entrance nozzle. This method of air-quantity measurement was used because space restriction did not permit a satisfactory installation of an inlet-orifice tank. No measurements of the state of the air were made in the annular area of the test section immediately ahead of the inducer; instead the air state on entering the test section from the inlet pipe was computed on the assumption of isentropic change. The losses through the inlet ducting were too small to be a source of appreciable error.

Precision. - The measurements made in the discharge plane of the inducer were generally not so reliable for establishing true performance as measurements obtainable in standard supercharger tests (reference 2). The measurements were of necessity made in regions of disturbed flow and small changes in temperatures and pressures were involved. The consistency and reproducibility of results, however, show that the measurements gave a good representation of the performance.

The precision of all measurements, exclusive of turbulence effects on static and total pressures at the inducer discharge, is estimated to be within the following limits:

| | |
|---|---|
| Temperatures, °F | ±0.5 |
| Pressures, inch of mercury | ±0.02 |
| Inducer speeds, percent | ±0.5 |
| Air quantity, percent | ±2 |

## TESTS

The cast deep inducers were tested over a range of air flows from exhauster capacity to the point of flow breakdown at several speeds. Because the speeds of the cast inducers were limited by the strength of the castings, each of the cast inducers was first spin-tested at a speed slightly greater than the maximum test speed. Tests of the inducer cut from the conventional impeller were terminated by blade failure at an impeller tip speed of 1100 feet per second.

The test conditions are given in the following table:

| Inducer | Tip speed, ft/sec | |
|---|---|---|
| | Inducer | Equivalent for 12-inch diameter impeller |
| 4-inch, 24-blade, unfinished edge | 267 | 400 |
| | 400 | 600 |
| | 533 | 800 |
| 4-inch, 24-blade, rounded edge | 267 | 400 |
| | 400 | 600 |
| | 533 | 800 |
| 4-inch, 12-blade, rounded edge | 267 | 400 |
| | 400 | 600 |
| | 533 | 800 |
| 2-inch, 24-blade, rounded edge | 267 | 400 |
| | 400 | 600 |
| | 533 | 800 |
| | 667 | 1000 |
| From conventional impeller | 400 | 600 |
| | 533 | 800 |
| | 667 | 1000 |
| | 733 | 1100 |

## COMPUTATIONS

The discharge-velocity components and the pressure and the temperature distributions can be determined by the use of measurements obtained at the inducer exit. The entrance conditions also being known, a method of rating the inducer as a compressor is available. No exact method of rating an inducer according to tangential velocities can be formulated until the true effects of velocity variations on performance are established. The tangential velocities in these tests are shown for direct comparison with wheel rotation, and a slip-factor expression is used as an index of the total pressure-energy increase for the inducer considered as a compressor.

The performance calculations for standard supercharger tests (reference 3) could not be directly applied to data obtained at each radial station of the inducers because the air flow through an inducer is not necessarily steady at constant radius. A method of obtaining a weight-flow average was therefore necessary. Continuity could not be satisfied by taking the area of the discharge duct as the flow area at the discharge instrument station because mixing from the separate inducer passages was incomplete. If the flow area at the instrument station (1/2 in. from the inducer) is taken as the area at the inducer discharge, the calculated discharge weight flow checks the inlet measurement within 4 percent over most of the flow range. At the smallest and the greatest air flows, the error in this weight-flow calculation was as much as 10 percent, owing to disturbed flow at the extreme operating conditions. The following performance characteristics of the inducers are based on integrated averages of weight-flow functions calculated from measurements at the inducer discharge:

(1) Adiabatic efficiency $\eta_{ad}$:

$$\eta_{ad} = \frac{\left(T_{1_t}{}^{Y}\right)_{av}}{\left(T_{2_t} - T_{1_t}\right)_{av}}$$

in which

$$\left(T_{1_t}{}^{Y}\right)_{av} = \frac{\sum T_{1_t}{}^{Y} \rho_2 V_{2_A} (2\pi r - b) \Delta r}{\sum \rho_2 V_{2_A} (2\pi r - b) \Delta r}$$

$$\left(T_{2_t} - T_{1_t}\right)_{av} = \frac{\sum\left(T_{2_t} - T_{1_t}\right) \rho_2 V_{2_A} (2\pi r - b) \Delta r}{\sum \rho_2 V_{2_A} (2\pi r - b) \Delta r}$$

$$Y = \left(\frac{p_{2_t}}{p_{1_t}}\right)^{\frac{\gamma-1}{\gamma}}$$

where

T temperature, $^{o}R$

$\rho$ air density, pounds per cubic foot

V air velocity, feet per second

r radius, inches

b total thickness of blades at radius r, inches

p pressure, inches of mercury absolute

$\gamma$ ratio of specific heats for normal air (1.3947)

Subscripts:

1 conditions in inlet pipe

2 conditions at discharge of inducer at radius

t total or stagnation value

A axial component

ad adiabatic

av average

(2) Slip factor $f_s$:

$$f_s = \frac{\sum \frac{\left(12 V_{2_T}\right)}{r \omega} \rho_2 V_{2_A} (2\pi r - b) \Delta r}{\sum \rho_2 V_{2_A} (2\pi r - b) \Delta r}$$

where $\omega$ is the angular velocity of the inducer in radians per second and the subscript T denotes the tangential component.

(3) Excess temperature rise (temperature rise above that required for isentropic compression):

$$\left(T_{2_t} - T_{1_t}\right)_{av} - \left(T_{1_t}{}^{Y}\right)_{av}$$

The integrations required in these computations were accomplished by the mechanical integration of curves plotted from values obtained in the radial surveys at the inducer discharge.

The integrated average adiabatic efficiency permits a direct rating of the inducer as a compressor. The statement of excess temperature rise is a measure of the direct loss in the inducer and is an index of an additional direct loss that must occur in the impeller owing to the excess temperature rise in the inducer. The integrated average slip factor is not entirely satisfactory as a measure of wheel rotation inasmuch as velocities exceeding wheel rotation tend to balance low velocities. Pressure coefficients are not given because the slip factor $f_s$ was near unity and the pressure coefficient may be defined as $f_s \eta_{ad}$. The inducer performance is plotted with reference to the load coefficient $Q_1/n$, in cubic feet per revolution, where $Q_1$ is inlet-air volume in cubic feet per second and $n$ is inducer speed in revolutions per second.

## RESULTS AND DISCUSSION

### Cast Inducers of the Constant-Angular-Acceleration Family

The 4-inch, 24-blade inducer, unfinished entrance edges. - The tangential discharge velocities produced by the 4-inch, 24-blade inducer with unfinished entrance edges are shown in figure 6 for equivalent tip speeds of 400, 600, and 800 feet per second. The load coefficient $Q_1/n$ and the blade angle of attack $\alpha$ is shown for each test condition; the tangential velocity required for wheel rotation is represented by a solid line. The inducer produced tangential velocities approaching those of wheel rotation as design flow conditions were approached. Velocities definitely lower than those required for wheel rotation were evident near the wall, especially at high flows. This characteristic was common to all the inducers of the constant-angular-acceleration family. The nature of the flow in the clearance at the inducer tip partly explains this change. The surveys at the inducer entrance showed no evidence of

prerotation at any point along the inducer radius until the tip was reached. At the tip the air had rotation in the direction of inducer rotation, probably as a result of backflow through the inducer clearance. The apparent decrease in rotation at the outer radii may also include a frictional loss of tangential velocity in the 1/2-inch distance from the inducer to the instrument station.

The rotation tended to break down near the inducer hub at throttled flows (see fig. 6), starting at the hub and continuing outward as the flow was throttled. The final breakdown of flow was influenced by the balancing of a uniform back pressure in the test-rig collector against the radially distributed pressure gradient of the inducer discharge. When an inducer operates on an impeller, the radial pressure gradient will not be subjected to this artificially imposed change in pressure distribution. The breakdown of flow observed in these tests is not indicative of the actual inducer-impeller combination.

The tangential-velocity characteristics at the three speeds shown for this inducer have a marked similarity. Because the rotational-velocity patterns of each of the inducers were generally independent of speed, the tangential-velocity curves for the other inducers are shown for only one speed.

The adiabatic efficiency, the excess temperature rise, and the slip factor at equivalent tip speeds of 600 and 800 feet per second are shown in figure 7. The adiabatic-efficiency curves are very similar at the two speeds; each reaches a maximum of 73 percent at approximately the design load coefficient of 0.24. For each of the inducers, in fact, the adiabatic-efficiency curves showed a marked similarity at all tip speeds with a practically constant peak efficiency. The slip factor approached unity for all conditions and showed a tendency to drop slightly as the flow deviated from the design load coefficient.

The 4-inch, 24-blade inducer, rounded entrance edges. - Tangential-velocity curves were similar at all test speeds for the 4-inch, 24-blade, rounded-edge inducer; the curves for 800 feet per second equivalent tip speed (fig. 8) are shown as representative. A comparison with the corresponding curves for the 4-inch, 24-blade, unfinished-edge inducer (fig. 6(c)) shows that the rotational characteristics are very similar and that the rounded entrance edges of the blades had no effect on the tangential velocities.

Axial discharge velocities for the rounded-edge inducer at an equivalent tip speed of 800 feet per second are presented in figure 9. These curves show that the breakdown of air flow near the

blade tips and the blade roots was more marked in axial velocity than in tangential velocity. The boundary layer in the inlet duct probably had an effect on the axial discharge velocity, but the variation in axial-velocity distribution through the range of load coefficients indicates the changing flow conditions through the inducer.

The performance characteristics for the 4-inch, rounded-edge inducer are shown for 600 and 800 feet per second equivalent tip speed in figure 10. The efficiency curves are similar and each reaches a peak value of approximately 80 percent near the design load coefficient. Rounding of the entrance edges of the blades resulted in an increase of 7 points in peak efficiency. Slip-factor curves are similar at both speeds and reach unity at the design load coefficient, as in the case of the inducer with unfinished edges. The effect of the blade rounding, therefore, was to increase the efficiency without changing the rotational characteristics.

Radial static-pressure distributions are shown in figure 11. These curves approach the parabolic form denoting wheel rotation but are modified by variations from wheel rotation. The ideal pressure gradient for wheel rotation is shown for a flow near the design point, with the ideal curve based on the measured pressure at the root-mean-square radius. Radial total-pressure distribution for selected weight flows are shown in figure 12. These pressure curves, shown only for this test, are representative of all the inducers.

The 4-inch, 12-blade inducer. - The characteristic tangential velocities of the 12-blade inducer were higher than wheel rotation at the hub and lower than wheel rotation at the outer radii (fig. 13). Near the design flow the velocity profiles approached wheel rotation but did not compare favorably with those of the 4-inch, 24-blade inducer. At throttled flows, the tangential velocities dropped below the values for wheel rotation, although the marked flow restriction near the hub was not present.

The adiabatic efficiency for the 4-inch, 12-blade inducer (fig. 14) was approximately 83 percent near a load coefficient of 0.28, dropping off to 60 percent in the range of a load coefficient of 0.20. The efficiency at 600 feet per second equivalent tip speed is shown to reach a maximum of about 92 percent at a load coefficient of 0.35 although the efficiency over most of the range checked the 800-foot curve. This marked difference, which did not occur with any other inducer, is possibly due to faulty test data.

Flow breakdown and an accompanying drop in efficiency occurred in the design range for this inducer. The range of audible surge is indicated on the curves. The average slip factor reached unity at approximately 0.22 load coefficient.

The 2-inch, 24-blade inducer. - A representative tangential-velocity plot for an equivalent tip speed of 800 feet per second is shown in figure 15 for the 2-inch, 24-blade inducer. At high flows the tangential velocities were similar to those of the 4-inch, 12-blade inducer, but at load coefficients near the design value the velocities over most of the blade length were higher than those required for wheel rotation.

The performance characteristics of the 2-inch inducer at equivalent tip speeds of 600, 800, and 1000 feet per second are shown in figure 16. The adiabatic-efficiency curves are similar at all speeds, with a peak value of approximately 78 percent near a load coefficient of 0.28. At each speed the inducer surged at a point slightly above the design load coefficient, with an accompanying drop in efficiency. The slip factors were below unity at high flows and above unity for low flows.

Blade loading and acceleration. - Comparative design data and performance data at an equivalent tip speed of 800 feet per second for the three inducers with rounded entrance edges are:

| Inducer | Design conditions | | | Performance characteristics | | | | |
|---|---|---|---|---|---|---|---|---|
| | Load coefficient (cu ft/ revolution) | Lift coefficient (at rms diam.) | Acceleration of air (radians/ $sec^2$) | Adiabatic efficiency $\eta_{ad}$ | | Slip factor $f_s$ | | Approach to wheel rotation[a] |
| | | | | At design $Q_1/n$ | Max. | At design $Q_1/n$ | Max. | |
| 4-inch, 24-blade | 0.24 | 0.43 | $2.16 \times 10^6$ | 0.78 | 0.80 | 1.00 | 1.00 | 1 |
| 4-inch, 12-blade | .24 | .86 | 2.16 | .60 | .82 | .99 | .99 | 2 |
| 2-inch, 24-blade | .24 | .86 | 4.32 | .67 | .79 | 1.04 | 1.06 | 3 |

[a]Comparative order in which tangential discharge velocities from the inducers approached wheel rotation.

The blade loading of inducers, which is a function of axial pressure gradient and flow per channel, has been shown by these limited tests to have an important influence on inducer performance. The 4-inch, 24-blade inducer had the lowest blade loading of the group and had the best air-rotational characteristics. At the design load coefficient the rotation of the discharged air was almost true wheel rotation. The 4-inch, 12-blade and the 2-inch, 24-blade inducers each had blade loadings twice as great as the 4-inch, 24-blade inducer. The rotational characteristics of these two inducers were quite similar, although the 4-inch, 12-blade inducer was slightly better, and their adiabatic efficiencies were very nearly alike over the entire test range. Each of these two inducers had a surge range at the design load coefficient and its highest efficiency at larger flows. They each had peak efficiences about the same as that of the 4-inch, 24-blade inducer but with inferior rotational characteristics.

The slightly better rotational characteristics produced by the 4-inch, 12-blade inducer than by the 2-inch, 24-blade inducer indicates that there may be an effect of the magnitude of acceleration, which is distinct from its direct function in blade loading. The angular acceleration of air for the 2-inch inducers is twice that for the 4-inch inducers. Conformity to wheel rotation decreased in the order of increasing passage area divergence along the mean flow path.

Lampblack flow patterns. - Lampblack flow patterns of the three rounded-edge inducers were made for air flows near the design load coefficient. The patterns showed the same general characteristics although the absolute dimensions varied slightly. A pattern on the pressure face of the 4-inch, 24-blade inducer was obtained at an equivalent tip speed of 800 feet per second at a load coefficient of 0.24 (fig. 17). This pattern showed a well-defined stagnation line that started at the blade tip at the entrance edge and constantly decreased in radius to 3.25 inches at the discharge end of the inducer blade. This stagnation line is probably the result of secondary flow existing in the inducer passage. The rotational-velocity curves for this inducer (fig. 8) show that at the 3.25-inch radius the tangential discharge velocity begins to decrease from that of wheel rotation.

The convex, or low-pressure, sides of the inducer blades had no pattern as definite as that on the pressure sides but triangular stagnation areas at the discharge blade tips were indicated on all the inducers. This pattern for the 2-inch, 24-blade inducer is shown in figure 18.

Inducer losses. - In an attempt to analyze the losses occurring in these inducers, calculations were made to determine approximate values for skin-friction losses and for mixing losses at the inducer discharge. These calculations, taking into account the varying hydraulic radius, the flow-path length, and the relative velocity through the inducer, were made for the 4-inch, 24-blade inducer at an equivalent tip speed of 800 feet per second. The mixing-loss calculation assumed a 100-percent loss of the kinetic-energy decrement in the enlargement from the inducer-passage discharge to the measurement station. The sum of these two calculated losses accounts for a loss of only $1\frac{1}{2}$ points in efficiency at peak efficiency and 4 points at a load coefficient of 0.34.

A more probable source of inducer losses is the entrance loss. Although no absolute method has been devised to determine the magnitude of this loss, figure 19 indicates the approximate entrance effect for the 4-inch rounded-edge inducer. The pressures shown were obtained from static-pressure wall taps and do not therefore represent the true conditions within the inducer. At the highest flow (high negative angle of attack); a static-pressure drop to a value of approximately 4 inches of mercury below the test-section pressure occurred in the first 3/4-inch axial depth of the 4-inch inducer. The pressure drop was nearly 1 inch of mercury at the design load coefficient even for the inducer with the rounded-edge entrance. At low flow, no pressure drop was apparent from the static-tap measurements. The marked increase in peak efficiency due to rounding the entrance edges of the blades (7 points in inducer efficiency) confirmed the importance of the entrance condition.

Additional losses in inducer performance probably result from secondary flow, turbulence, and separation. The extent of these losses was not determined, however, because of inadequate knowledge of the nature of inducer flow.

## Inducer Section from Conventional Impeller

The tests of the inducer section cut from the conventional impeller were made under the same conditions as the tests of the cast inducers of the constant-angular-acceleration family. The tangential-velocity curves for an equivalent tip speed of 800 feet per second (fig. 20) show an excess rotation characteristic similar to that of the 2-inch inducer of the constant-angular-acceleration family. The tangential velocities were greater than required for wheel rotation over most of the range but approached wheel rotation

at very low flow. The departures from wheel rotation are slightly greater than for the 2-inch inducer. As shown in figure 21, the slip factor for this inducer section was greater than unity over most of the flow range.

The adiabatic-efficiency curves at equivalent tip speeds of 800, 1000, and 1100 feet per second (fig. 21) are quite similar. The tests at equivalent tip speeds of 1100 feet per second are incomplete because of failure of the inducer. The efficiency increased with increasing flow quantity; the flow limit of the test equipment was reached without reaching a peak of inducer efficiency. This characteristic was logical for this bent-blade type of inducer because there is very little blade bending, particularly at the inner radii. The efficiency of this inducer was low over the entire operating range of the impeller of which it was a part. The efficiency of this inducer ranged from approximately 42 to 68 percent over its normal operating range; the efficiency of the 4-inch, 24-blade inducer over the same flow range was above 70 percent.

## Estimate of Inducer Effect

Calculations were made to estimate the possible effect of substituting one of the deep inducers in place of a bent-bucket section on an impeller. The bent-bucket section of the conventional impeller, which (remachined to constant diameters) had been tested, was assumed to be replaced by a deep inducer on the same impeller. These calculations are considered to indicate possible orders of magnitude and not absolute values because the necessary assumptions are not entirely valid and do not reflect actual conditions. The assumptions are that the performance of the inducers with an impeller would remain the same as their performance as separate components and that the impeller proper would function the same for any inducer. This comparative calculation is based on unpublished test data of a supercharger incorporating the conventional impeller. The peak efficiency of this supercharger at a tip speed of 800 feet per second occurred near the load coefficient for maximum efficiency of the 4-inch, 24-blade inducer as a separate component; but the efficiency of the bent-bucket section of the impeller, tested separately, was quite low at this load coefficient. Under these stated assumptions, substitution of the 4-inch, 24-blade inducer indicated a gain of 10 points in efficiency at an impeller tip speed of 800 feet per second and substitution of the 2-inch, 24-blade inducer indicated an increase of 6 points in maximum efficiency.

## SUMMARY OF RESULTS

Tests of three cast deep inducers (one with two entrance-edge forms) and a bent-bucket inlet section cut from a conventional impeller established the following results:

1. Large differences in efficiency of inducers as separate components are shown to exist.

2. A 4-inch, rounded-edge inducer with 24 blades produced a near approach to wheel rotation with a peak adiabatic efficiency of 80 percent at a flow quantity near the design load coefficient.

3. The peak inducer efficiency was raised 7 points above that obtained with unfinished entrance edges by rounding the entrance edges of the blades of a 4-inch, 24-blade inducer.

4. A 2-inch inducer, a 4-inch, 12-blade inducer, and a bent-bucket inlet section all produced further departure from wheel rotation than a 4-inch, 24-blade inducer.

5. The adiabatic efficiency of the inducer section from the conventional impeller was low in the range of peak performance of the cast inducers and of the impeller of which it was a part. The adiabatic efficiency of this bent-bucket inlet section increased with increasing flow over the entire range of tests.

Aircraft Engine Research Laboratory,
National Advisory Committee for Aeronautics,
Cleveland, Ohio.

## REFERENCES

1. von der Nüll, Werner: The Design of Airplane-Engine Superchargers. NACA TM No. 839, 1937.

2. Ellerbrock, Herman H., Jr., and Goldstein, Arthur W.: Principles and Methods of Rating and Testing Centrifugal Superchargers. NACA ARR, Feb. 1942.

3. NACA Subcommittee on Supercharger Compressors: Standard Procedures for Rating and Testing Centrifugal Compressors. NACA ARR No. E5F13, 1945.

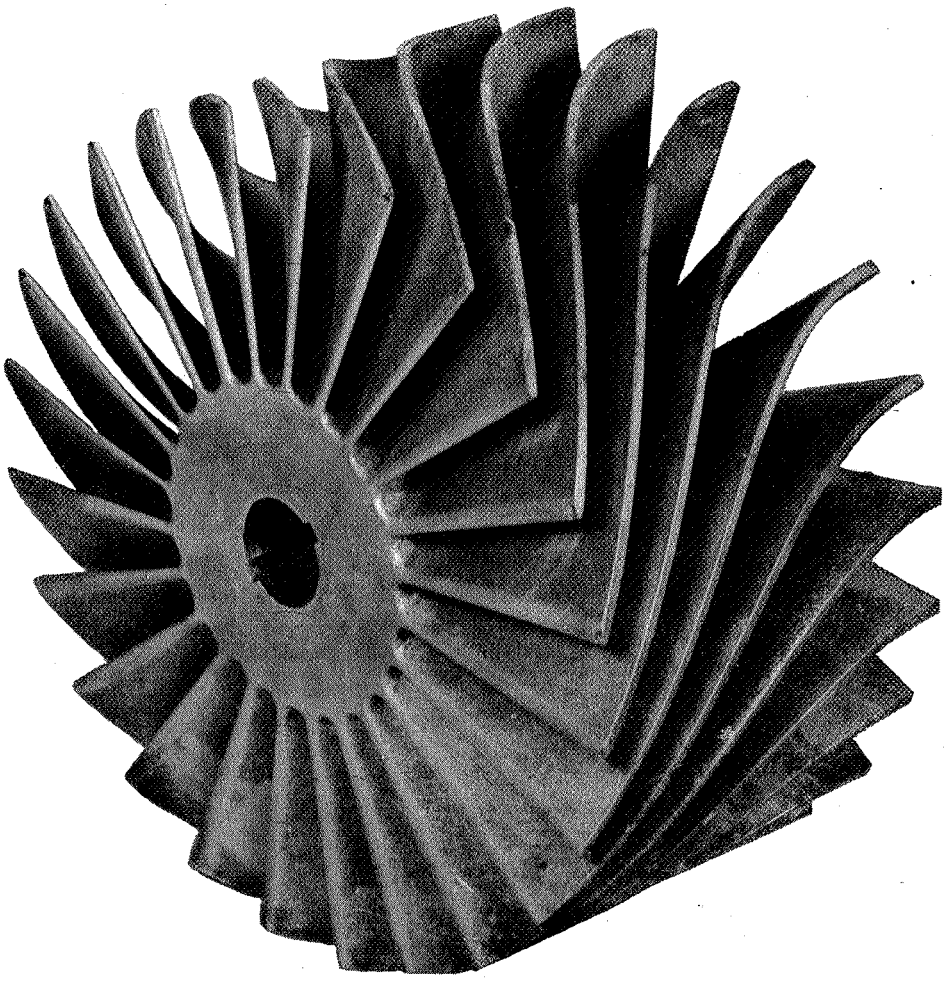


Figure 1. - The 4-inch, 24-blade cast deep inducer with rounded entrance edges.

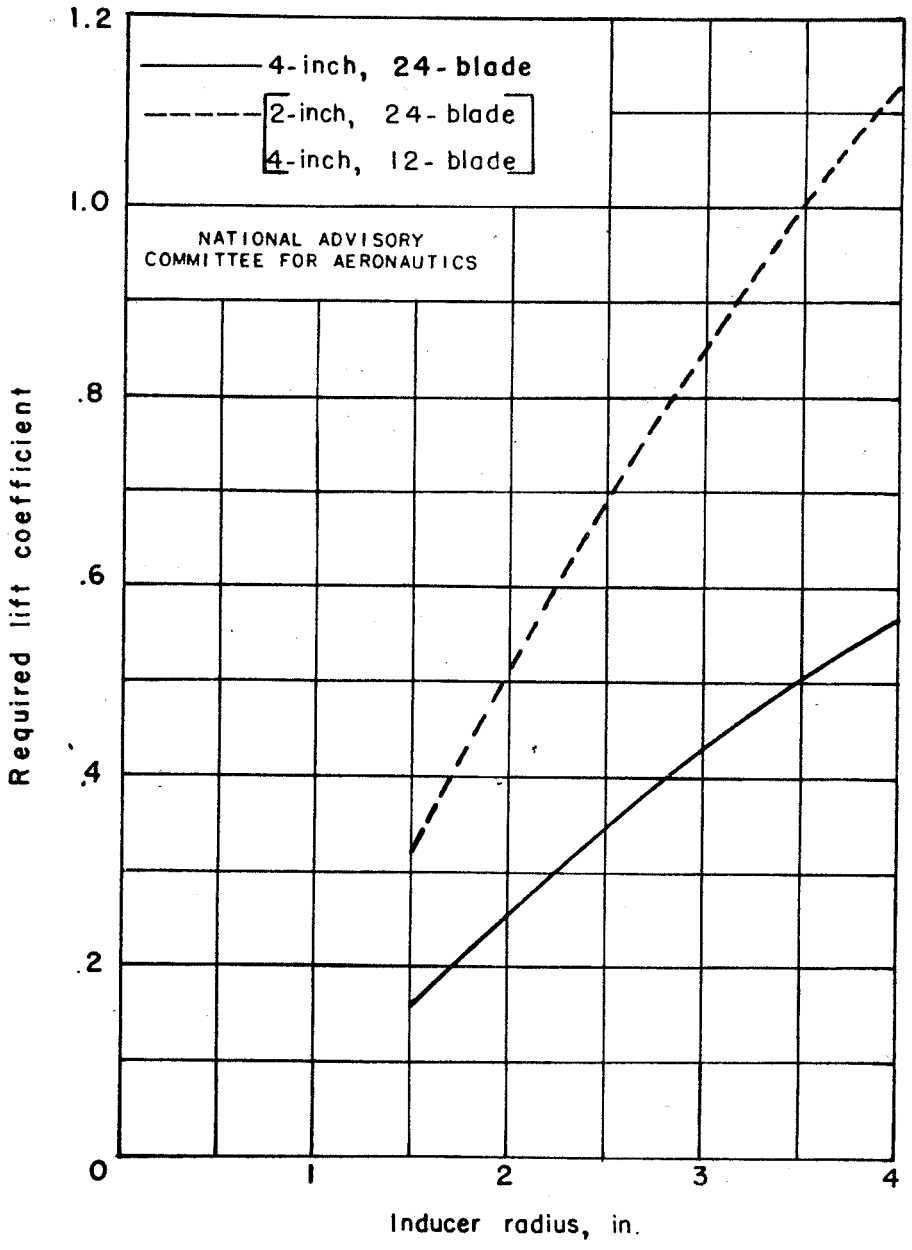


Figure 2.— Lift coefficient required to induce wheel rotation in three constant-angular-acceleration inducers.

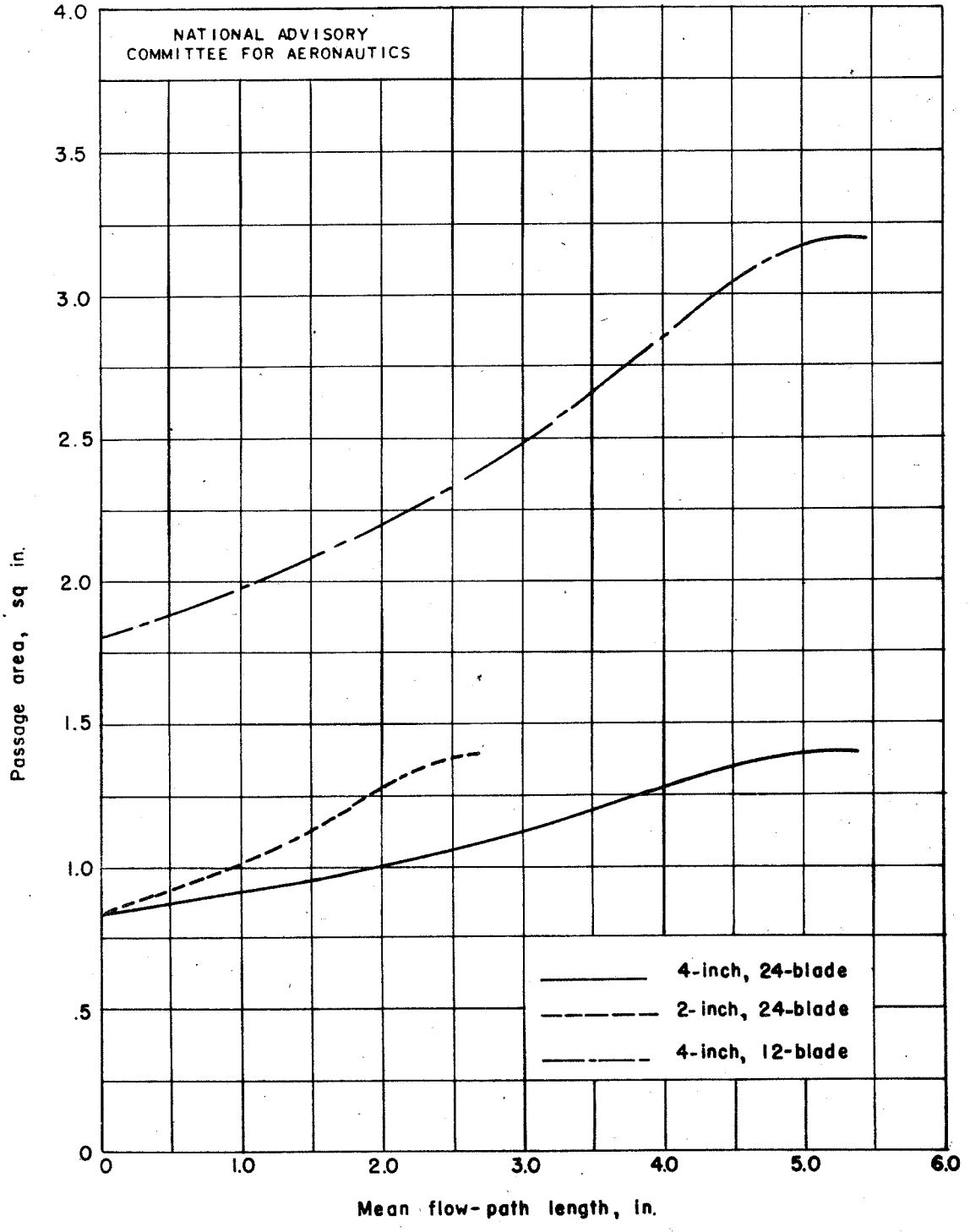


Figure 3.— Passage area of cast deep inducers.

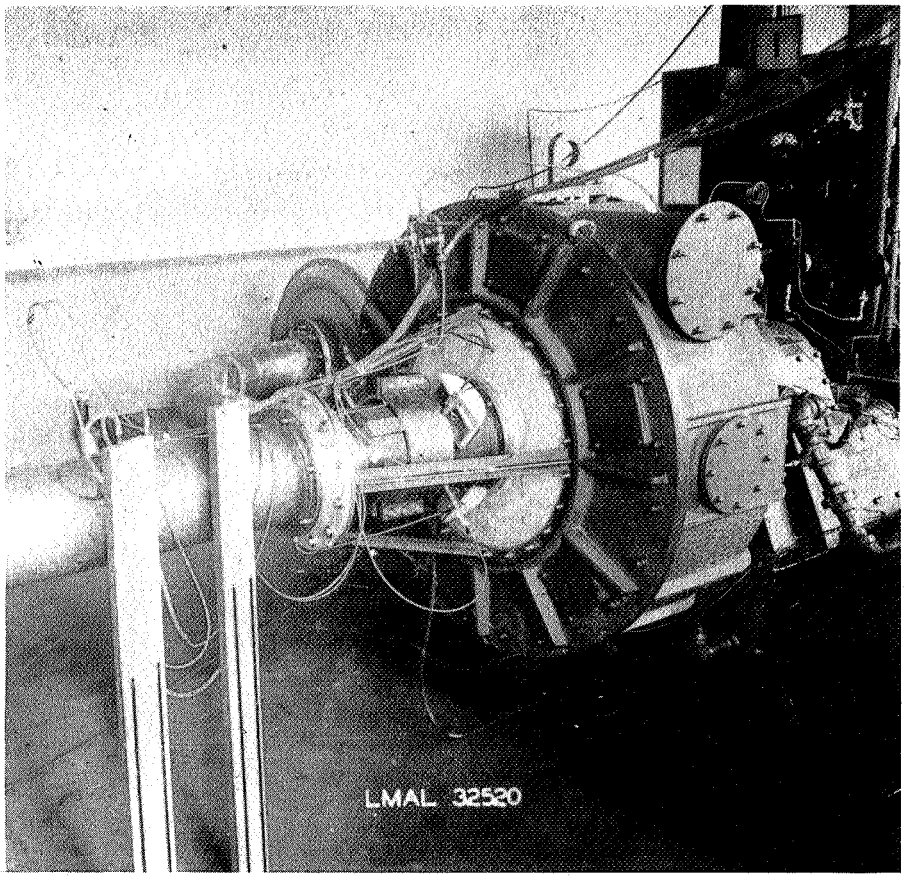


Figure 4. - Variable-component test rig adapted for inducer tests.

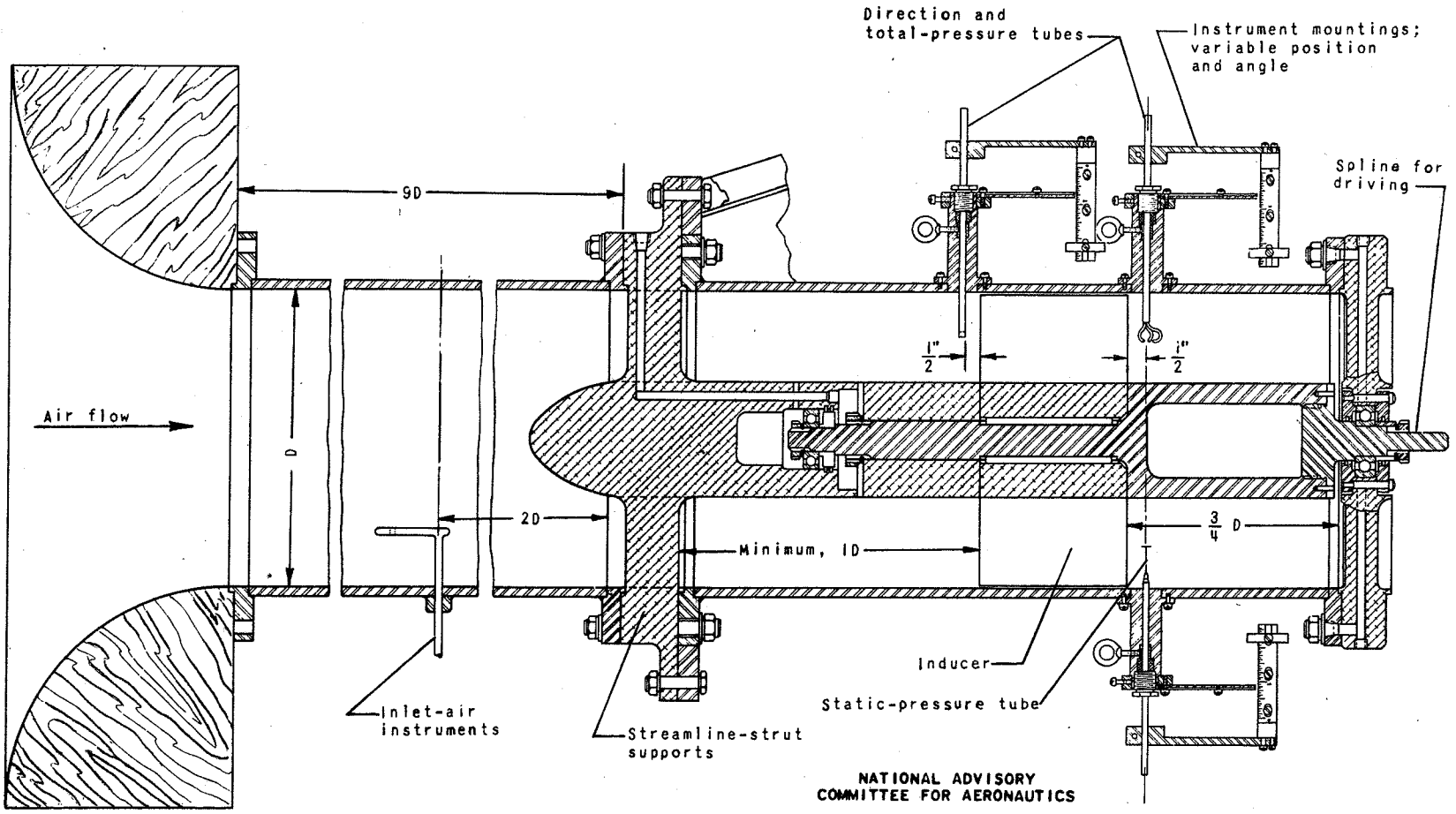


Figure 5. - Inducer test section showing location of pressure-measuring and temperature-measuring instruments.

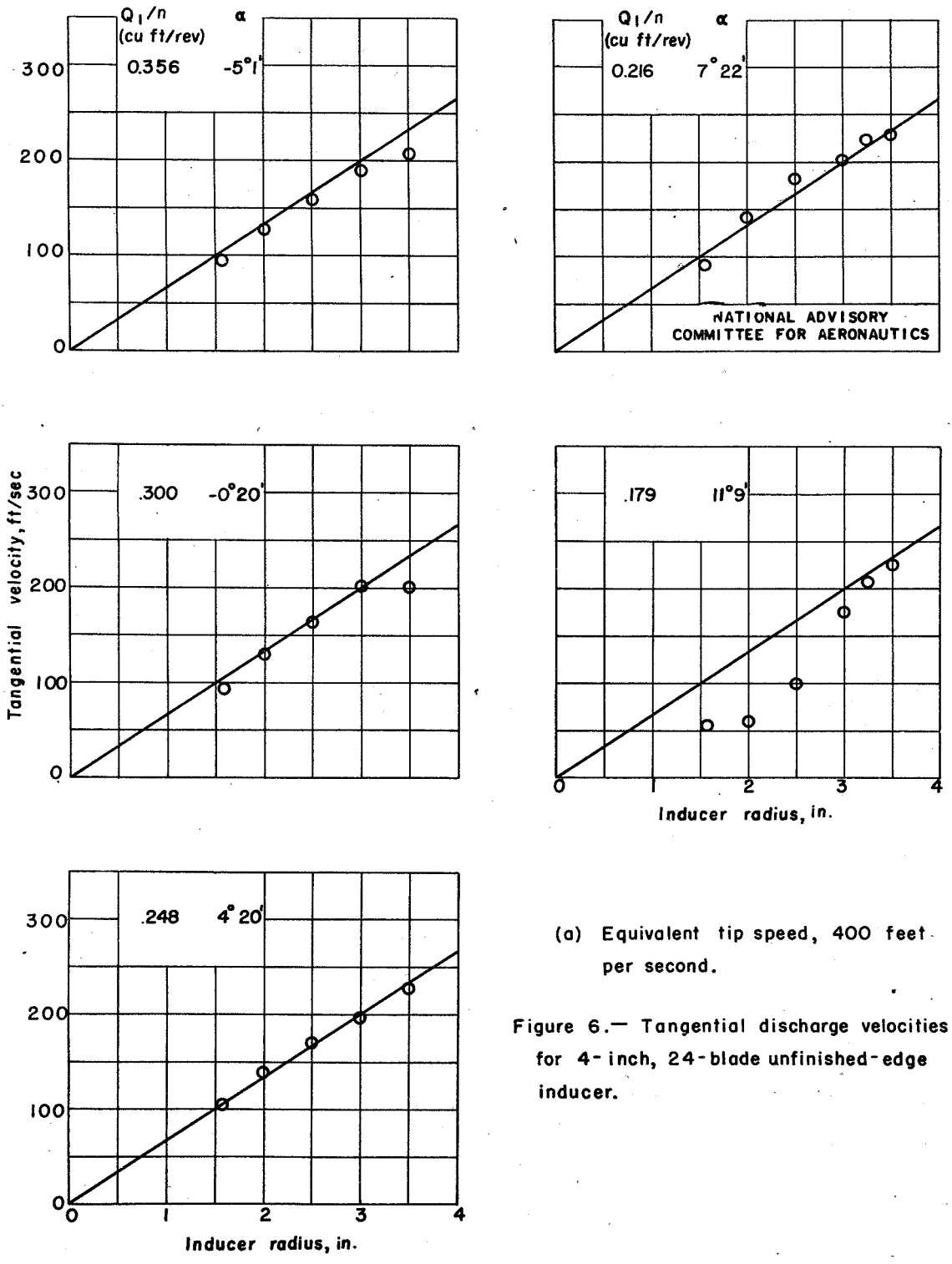


(a) Equivalent tip speed, 400 feet per second.

Figure 6.— Tangential discharge velocities for 4-inch, 24-blade unfinished-edge inducer.

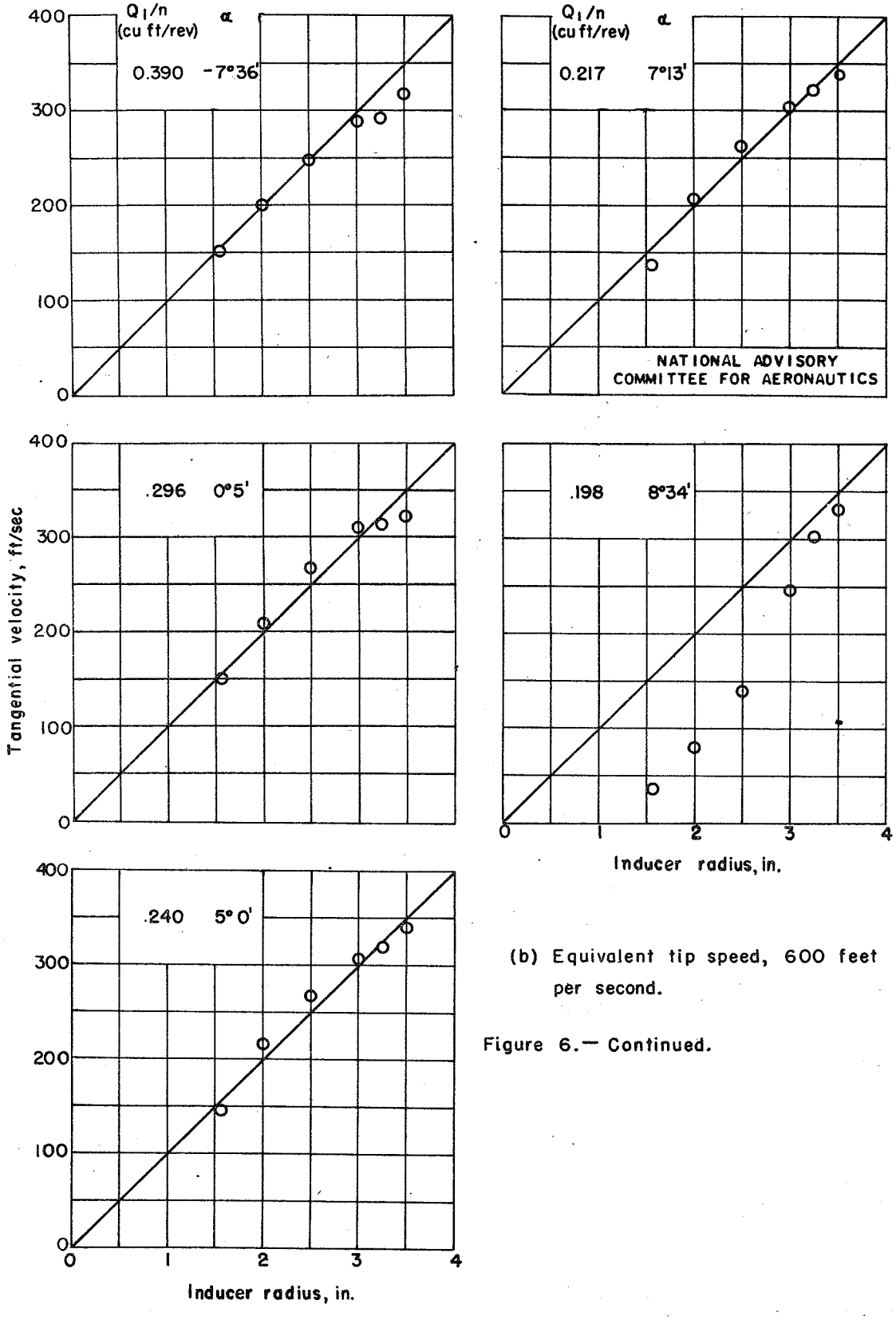


(b) Equivalent tip speed, 600 feet per second.

Figure 6.— Continued.

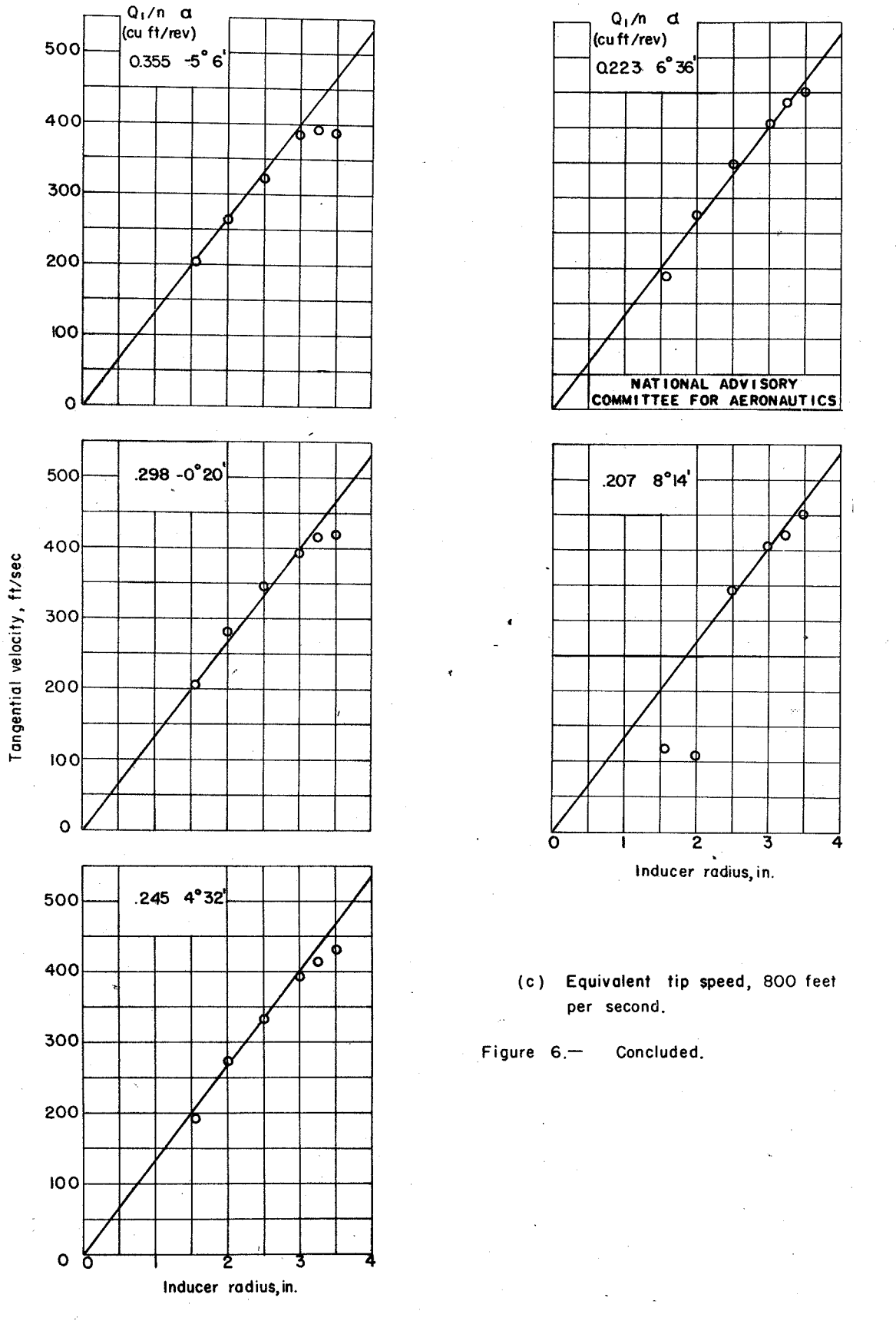


(c) Equivalent tip speed, 800 feet per second.

Figure 6.— Concluded.

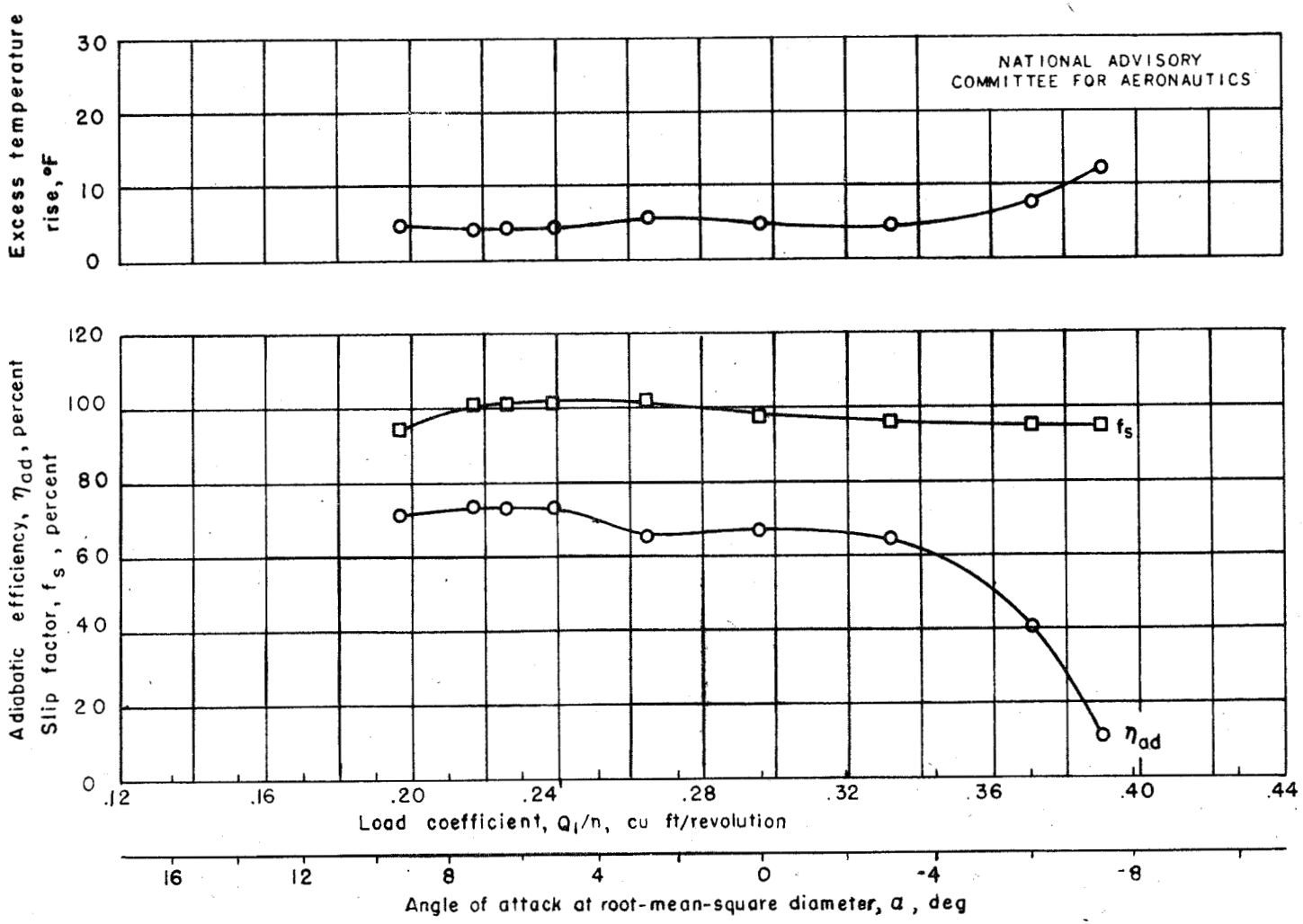


(a) Equivalent tip speed, 600 feet per second.

Figure 7.— Performance characteristics of 4-inch, 24-blade, unfinished-edge inducer.

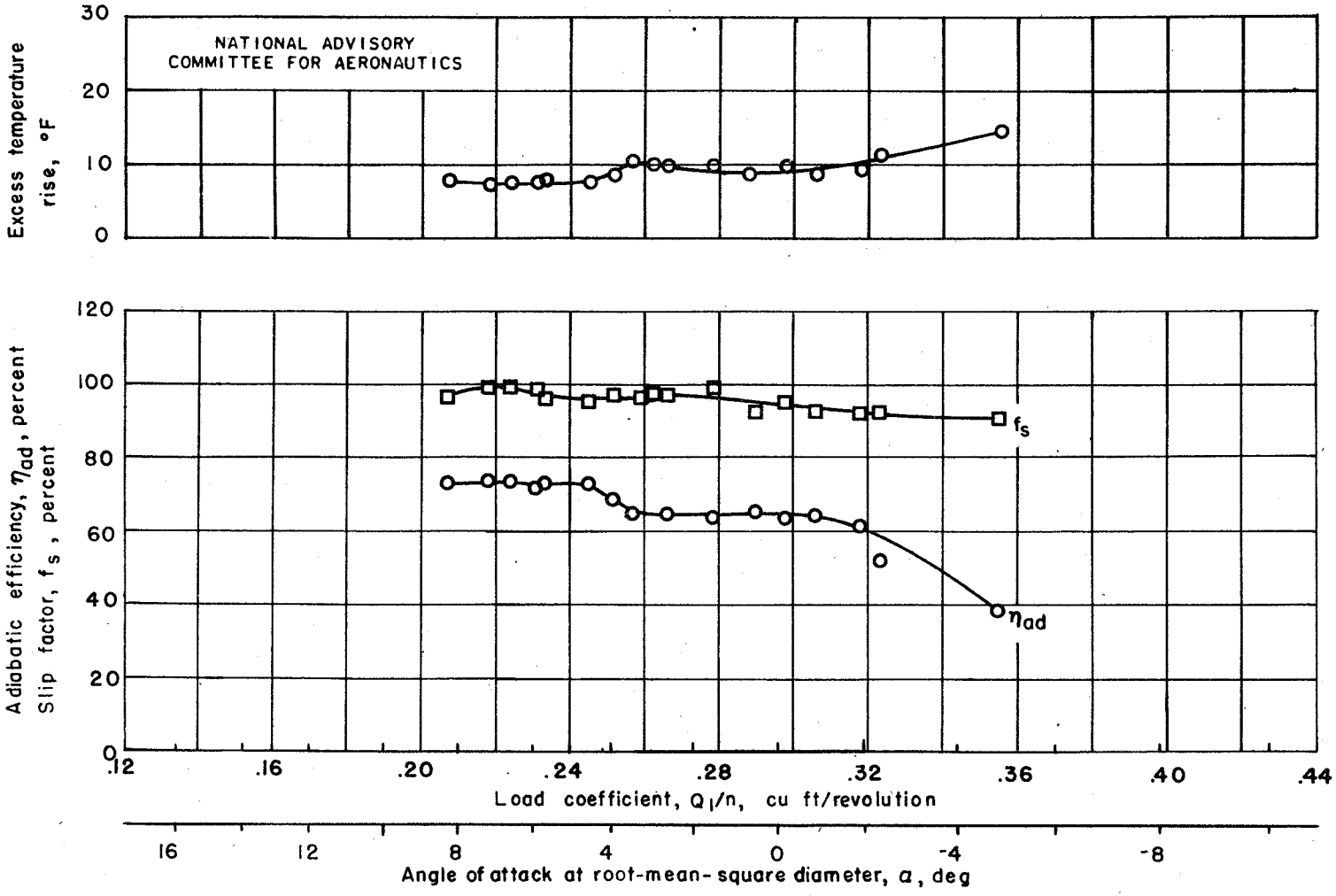


(b) Equivalent tip speed, 800 feet per second.

Figure 7.— Concluded.

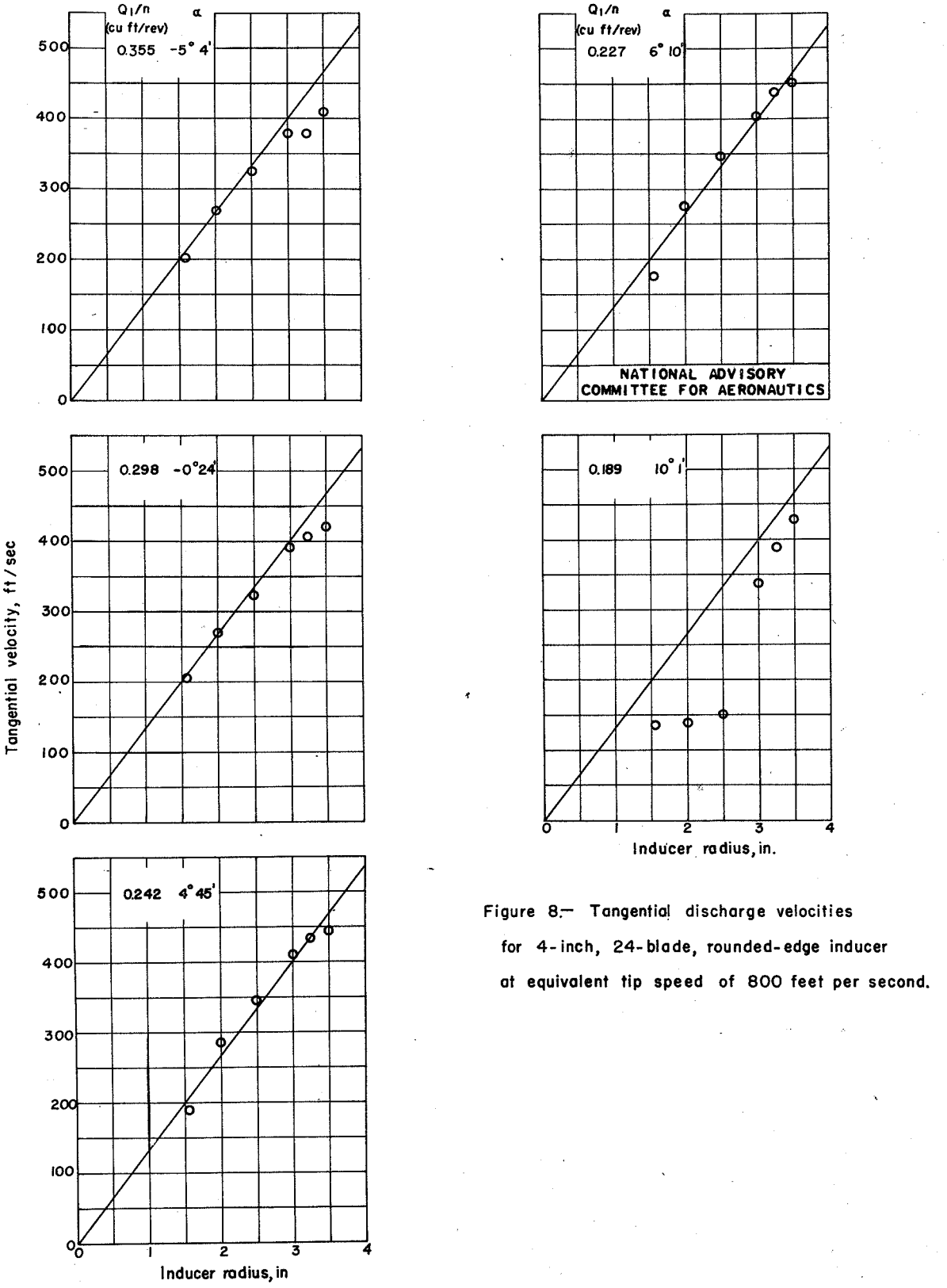


Figure 8.— Tangential discharge velocities for 4-inch, 24-blade, rounded-edge inducer at equivalent tip speed of 800 feet per second.

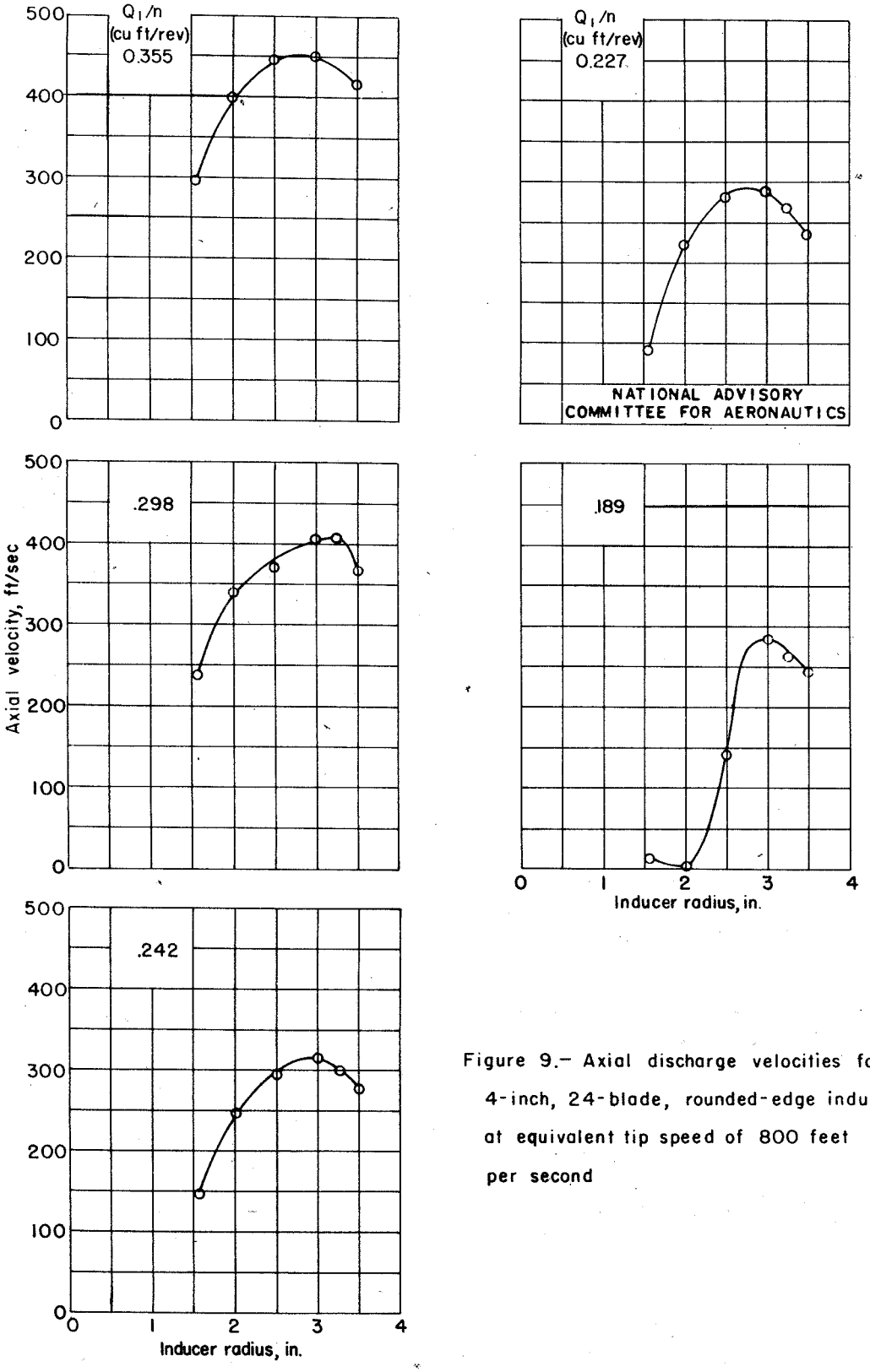


Figure 9.– Axial discharge velocities for 4-inch, 24-blade, rounded-edge inducer at equivalent tip speed of 800 feet per second

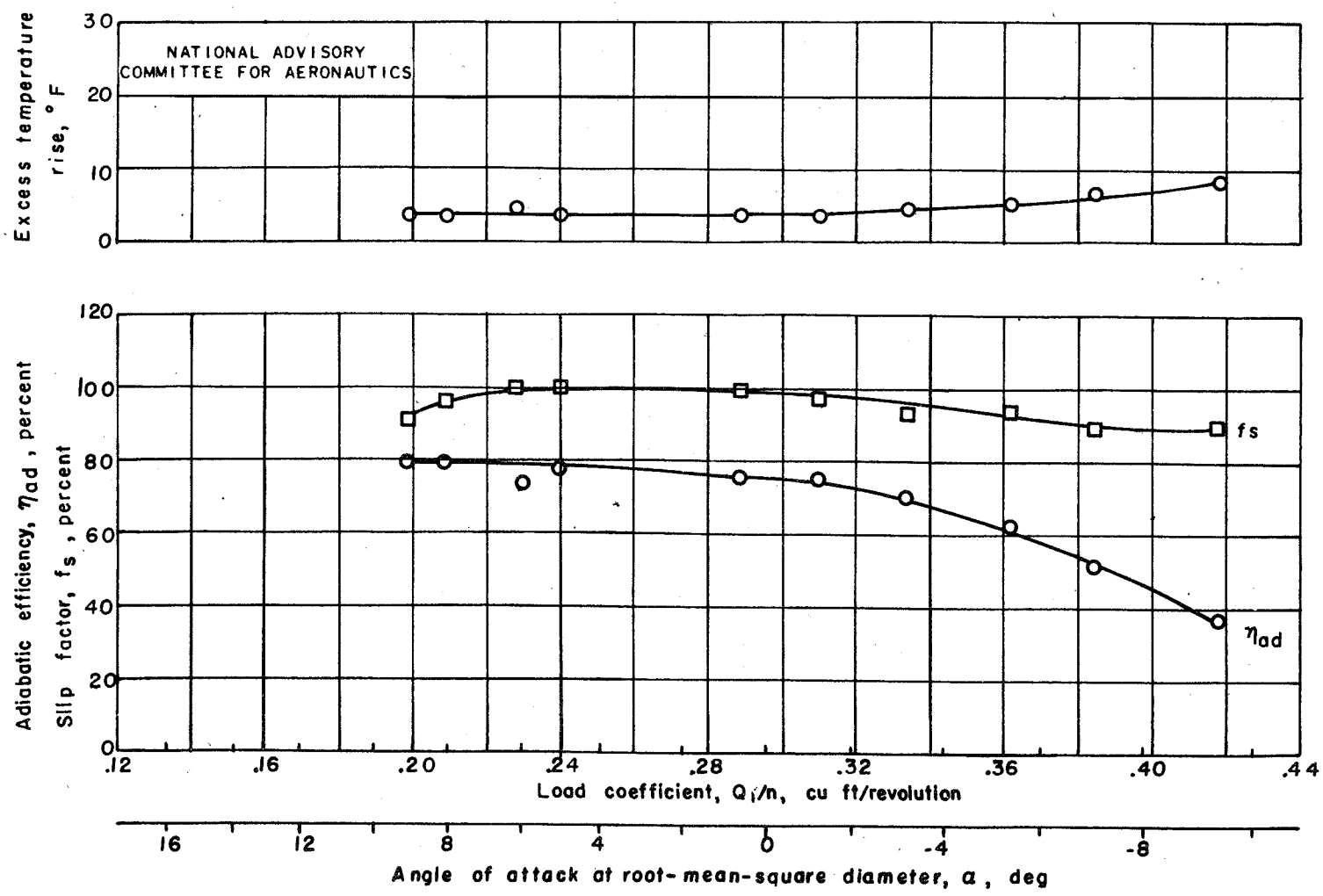


(a) Equivalent tip speed, 600 feet per second.

Figure 10.— Performance characteristics of 4-inch, 24-blade, rounded-edge inducer.

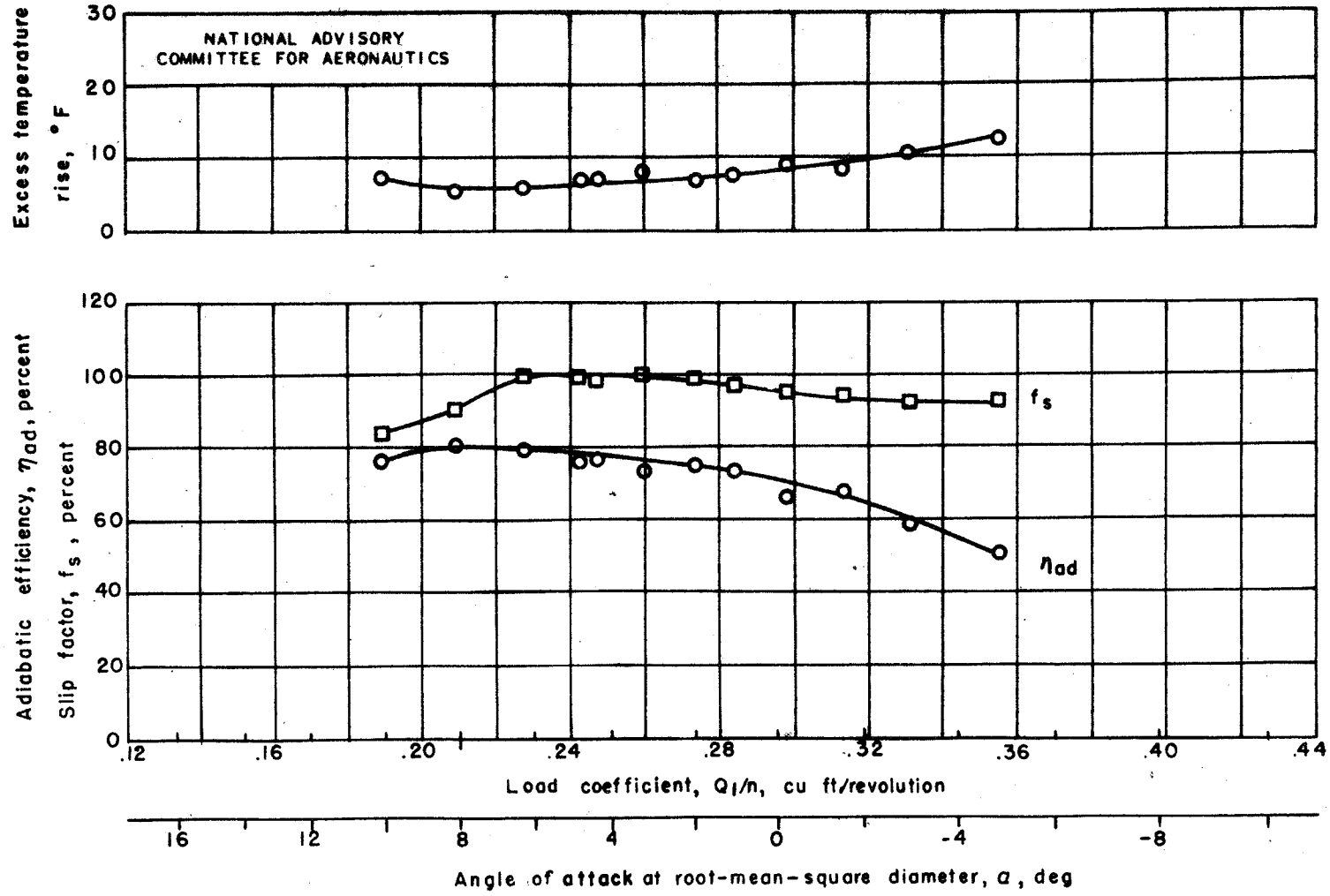


(b) Equivalent tip speed, 800 feet per second.

Figure 10.– Concluded.

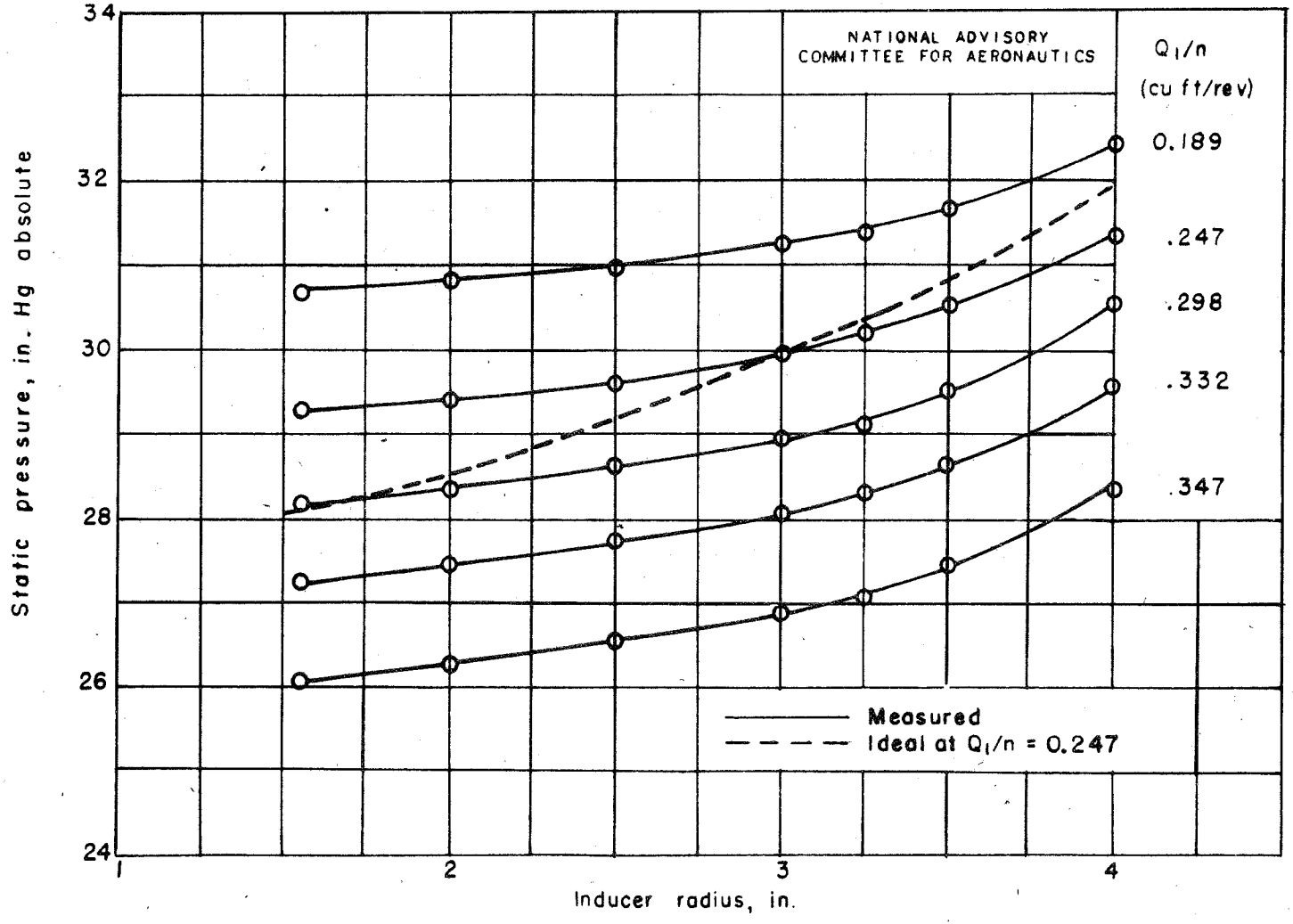


Figure 11.— Static pressure at discharge of 4-inch, 24-blade, rounded-edge inducer at equivalent tip speed of 800 feet per second.

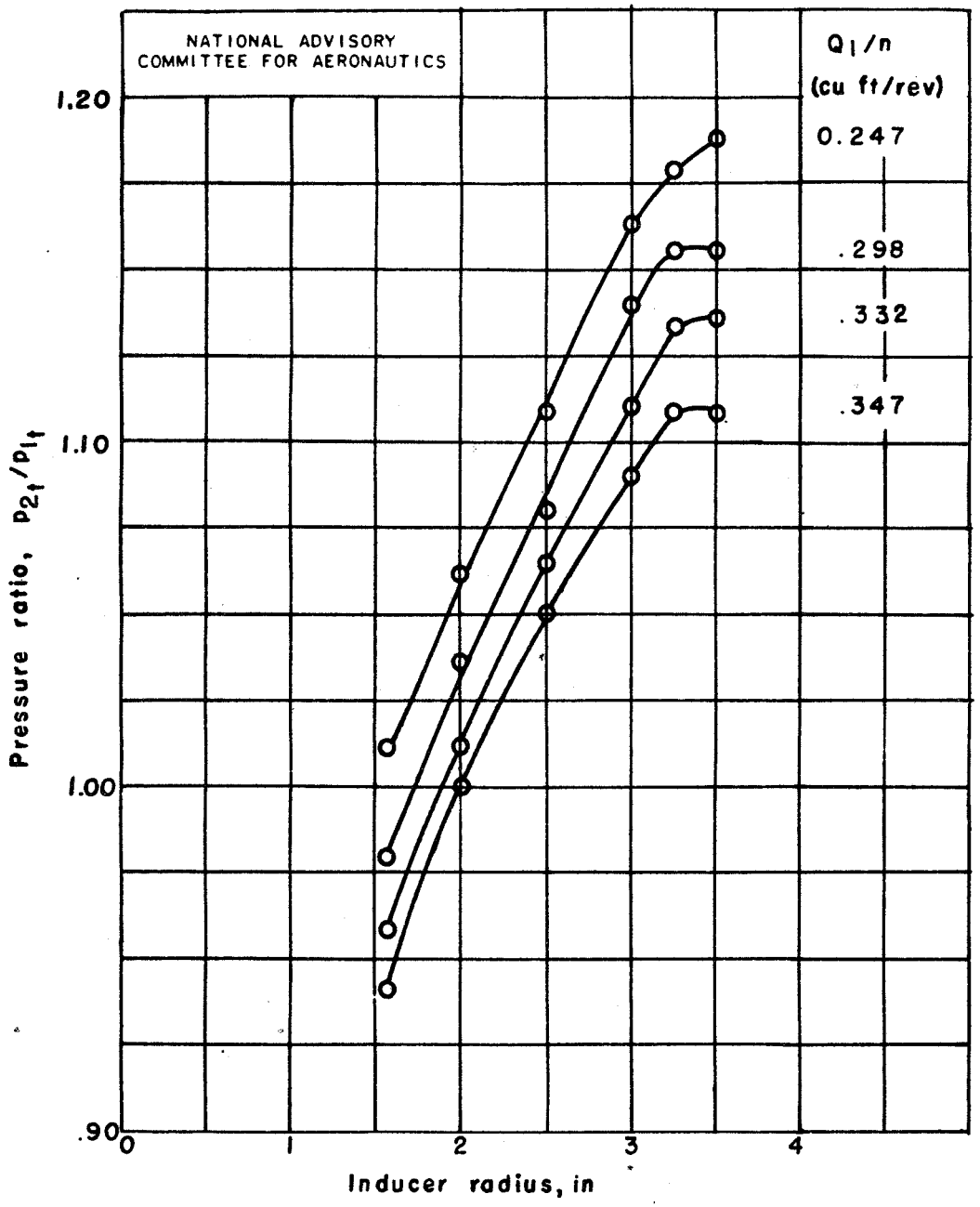


Figure 12.– Total-pressure distribution in 4-inch, 24-blade, rounded-edge inducer at equivalent tip speed of 800 feet per second.

Fig. 13

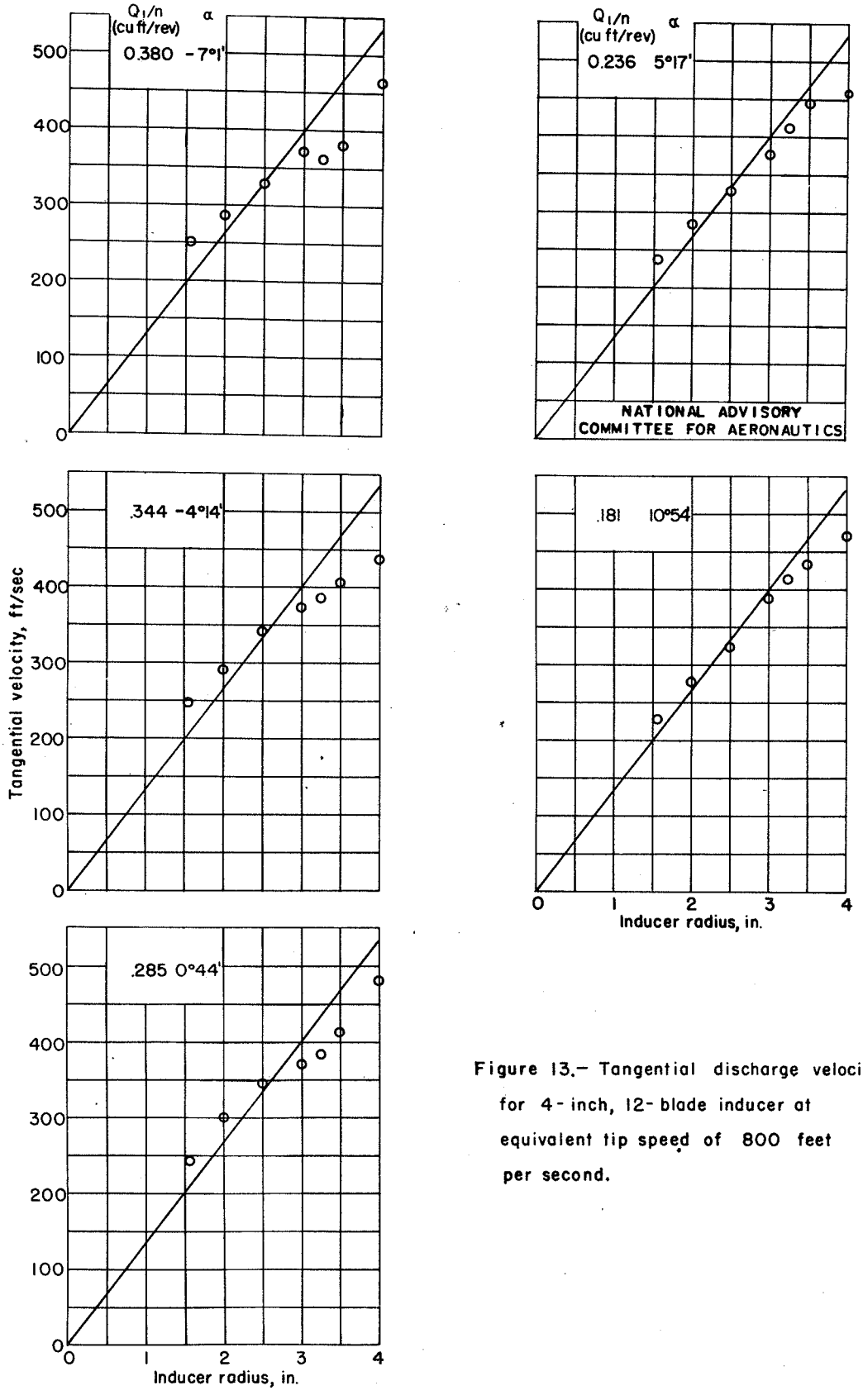


Figure 13.– Tangential discharge velocities for 4-inch, 12-blade inducer at equivalent tip speed of 800 feet per second.

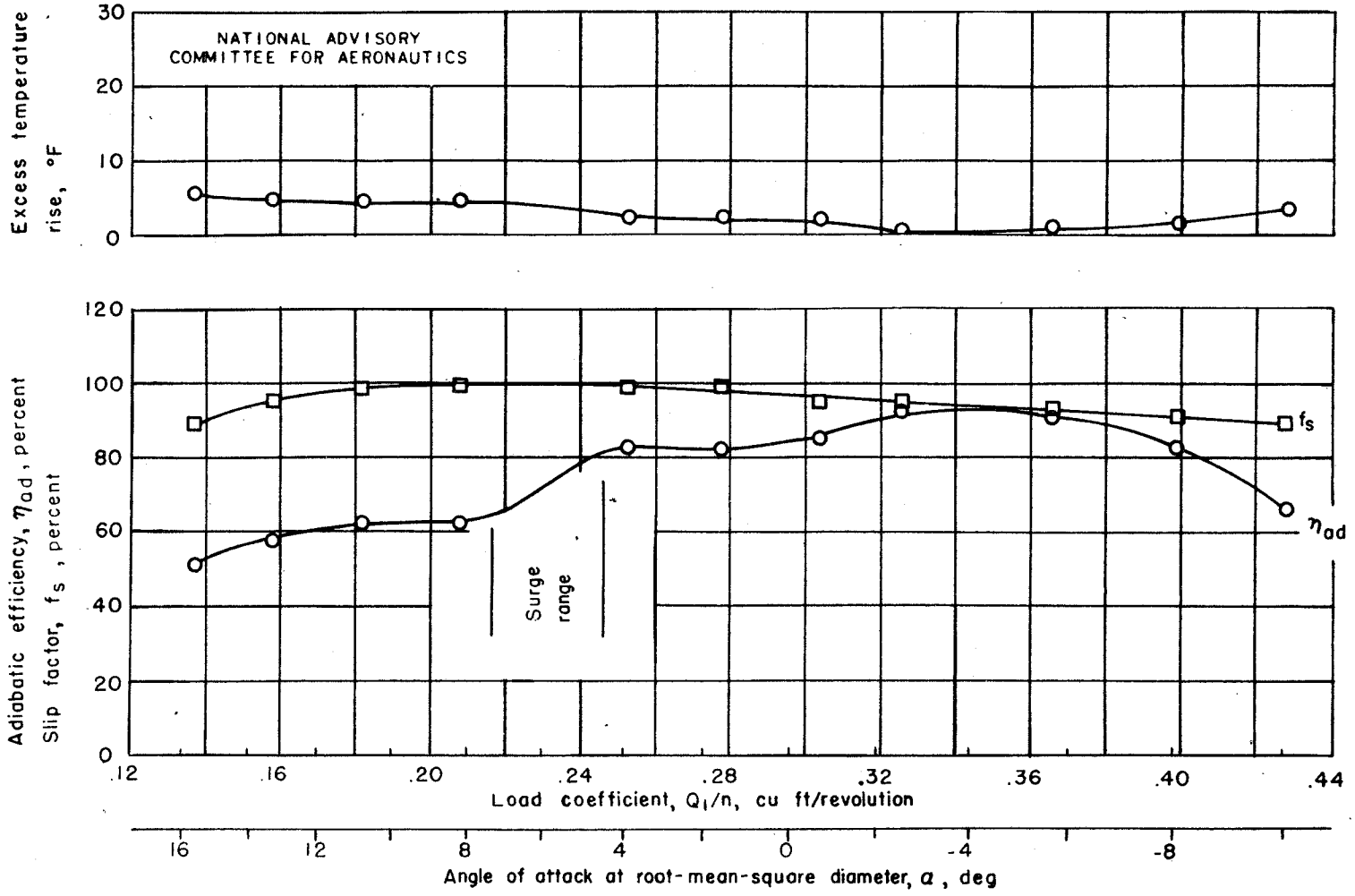


(a) Equivalent tip speed, 600 feet per second.

Figure 14.— Performance characteristics of 4-inch, 12-blade inducer.

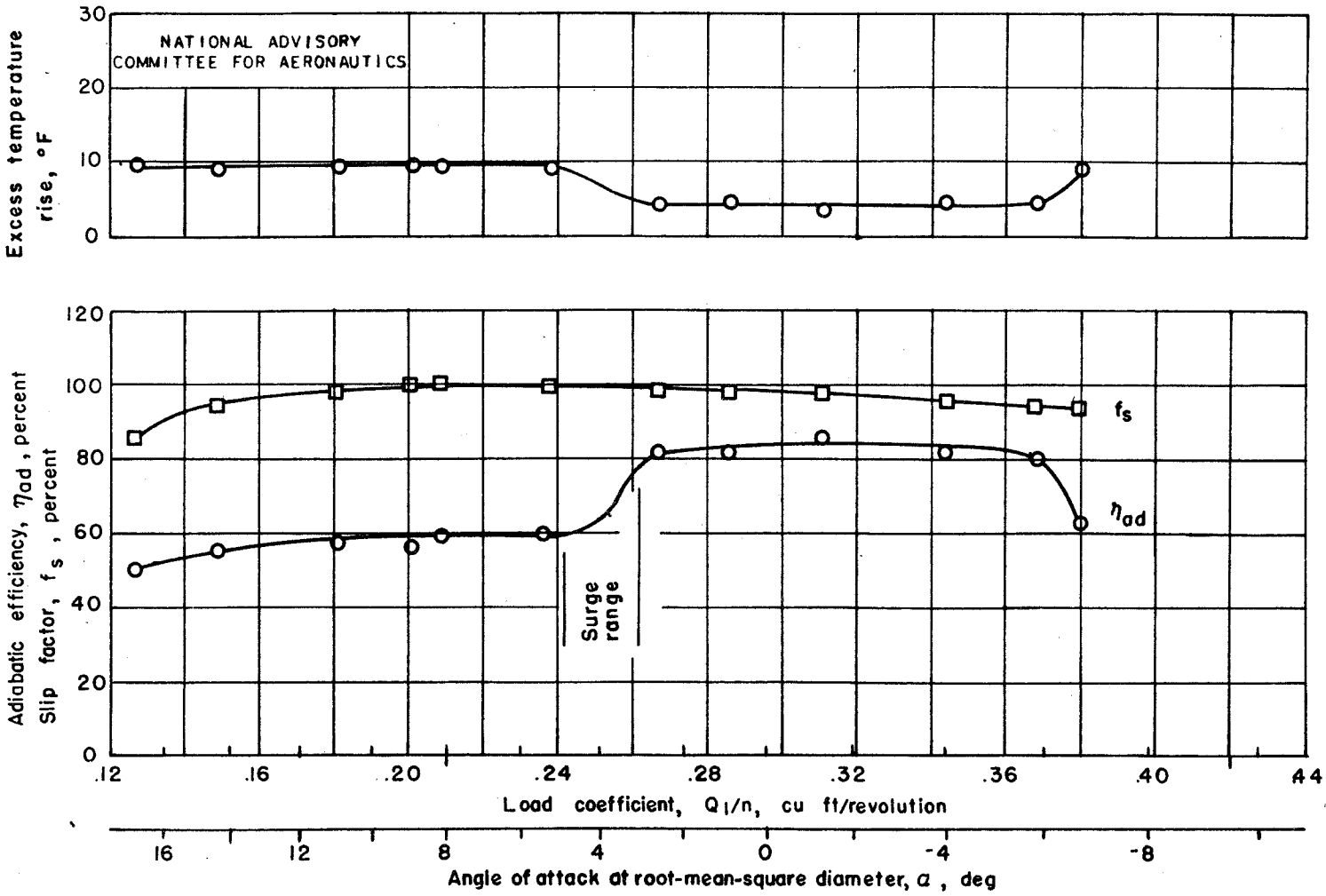


(b) Equivalent tip speed, 800 feet per second.

Figure 14.— Concluded.

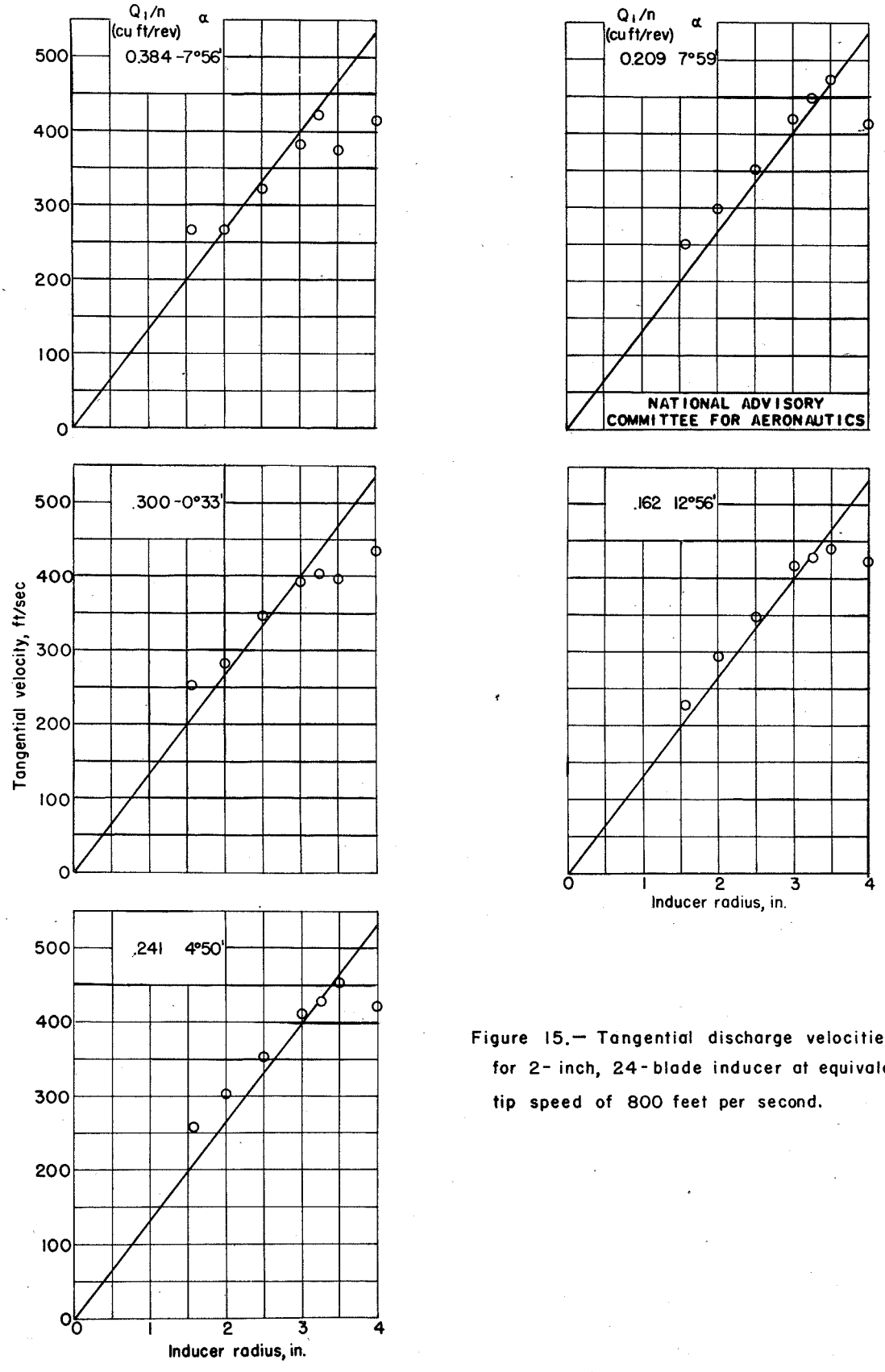


Figure 15.— Tangential discharge velocities for 2- inch, 24- blade inducer at equivalent tip speed of 800 feet per second.

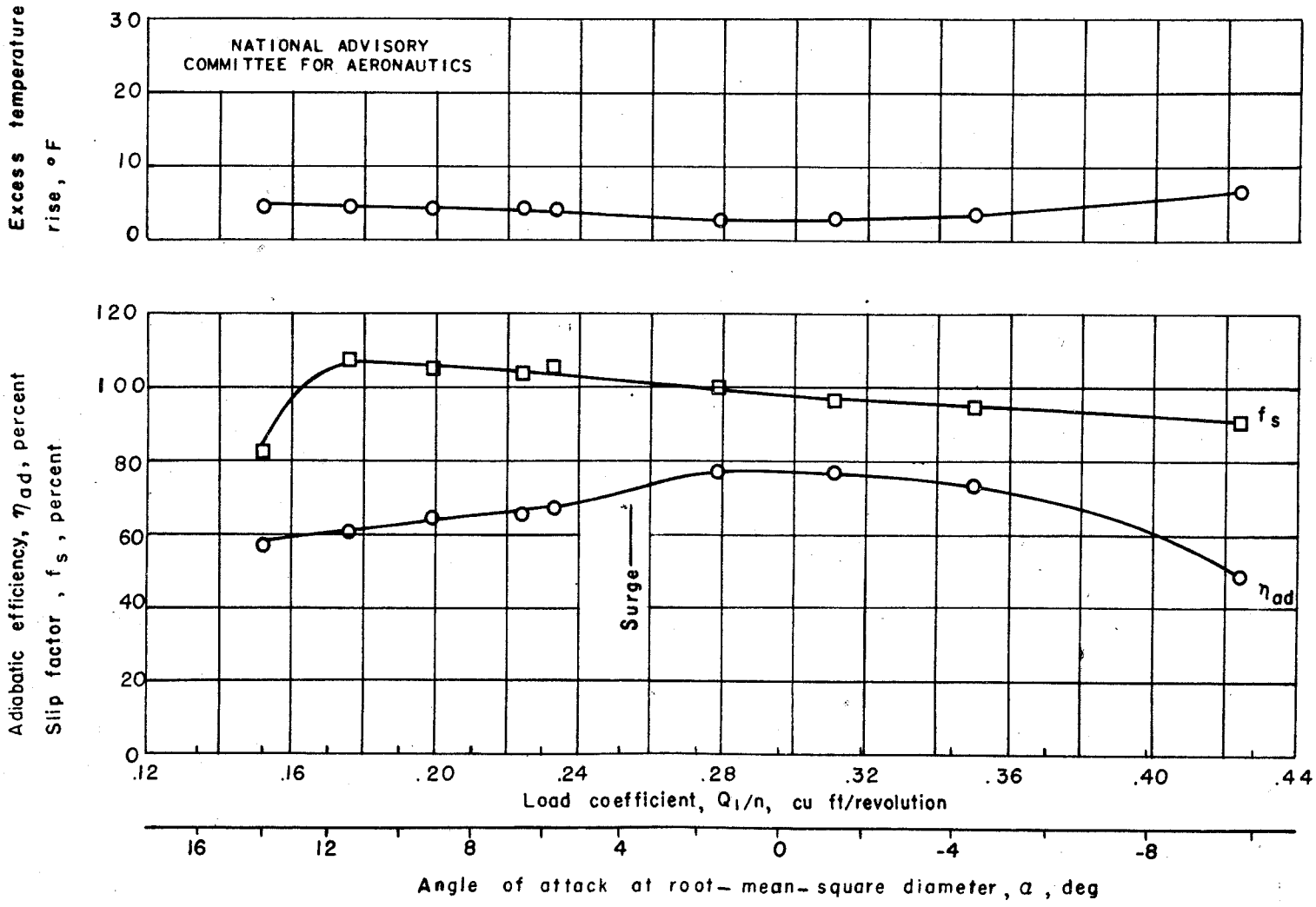


(a) Equivalent tip speed, 600 feet per second.

Figure 16.- Performance characteristics of 2-inch, 24-blade inducer.

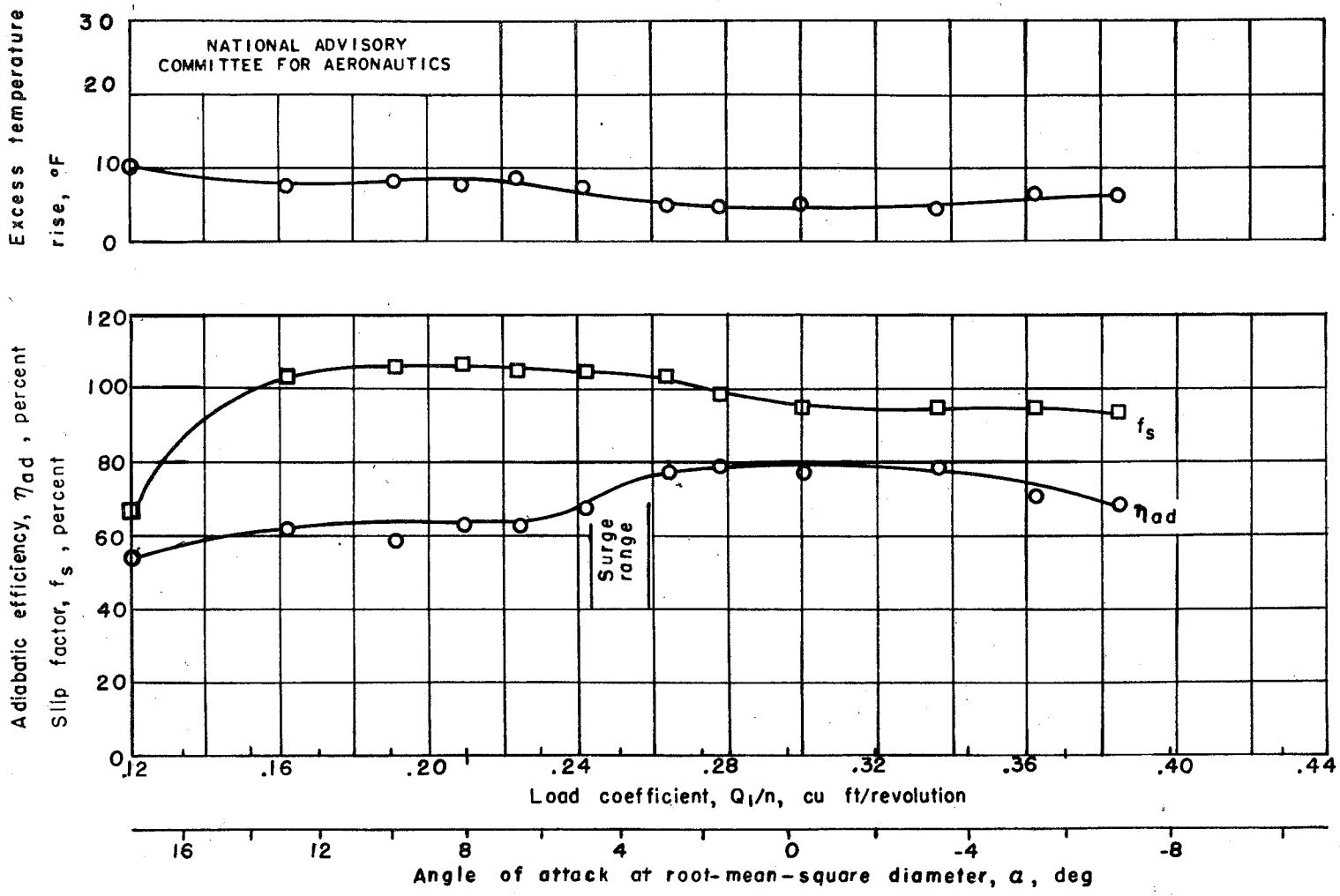


(b) Equivalent tip speed, 800 feet per second.

Figure 16.— Continued.

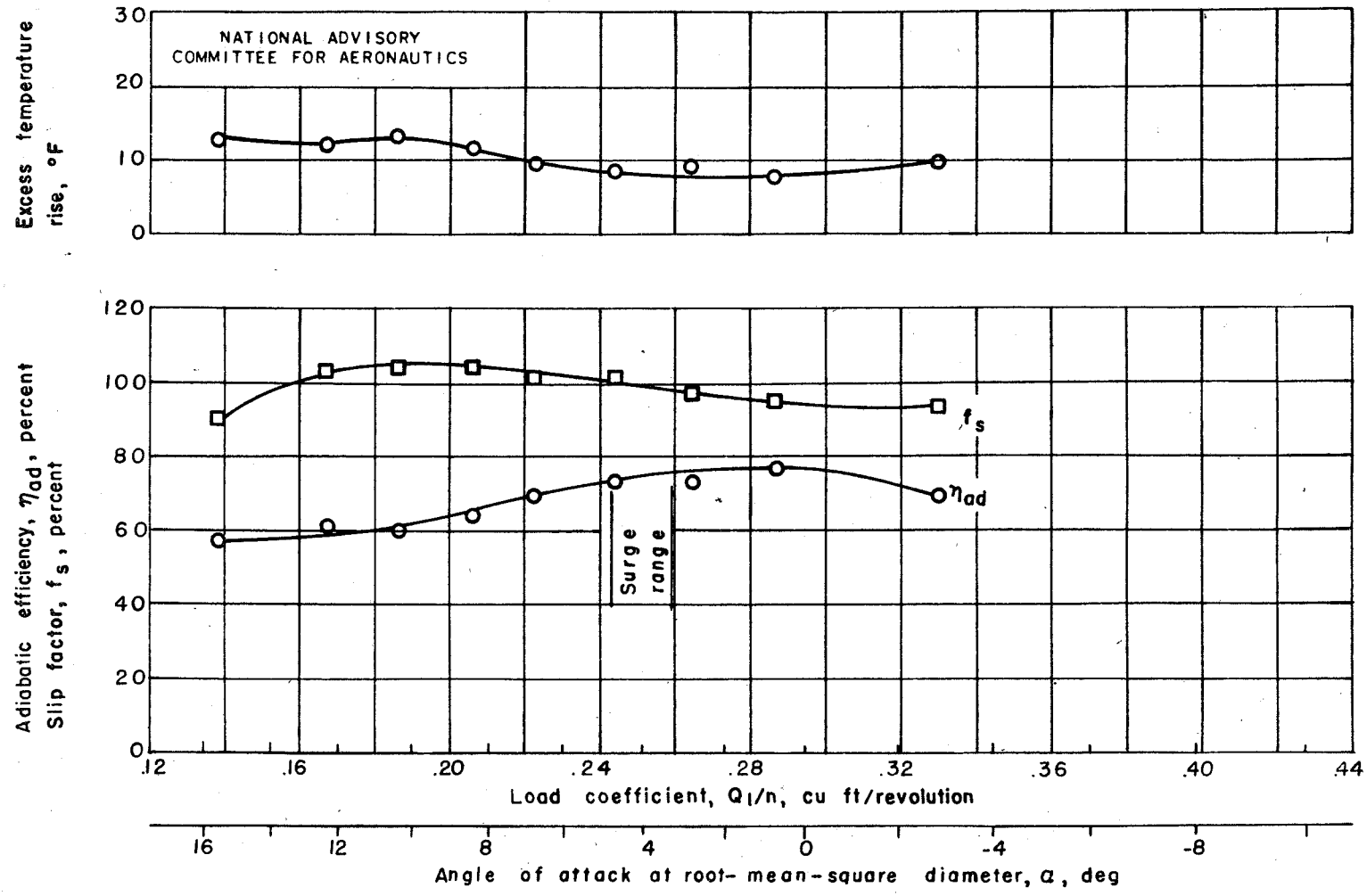


(c) Equivalent tip speed, 1000 feet per second.

Figure 16.— Concluded.

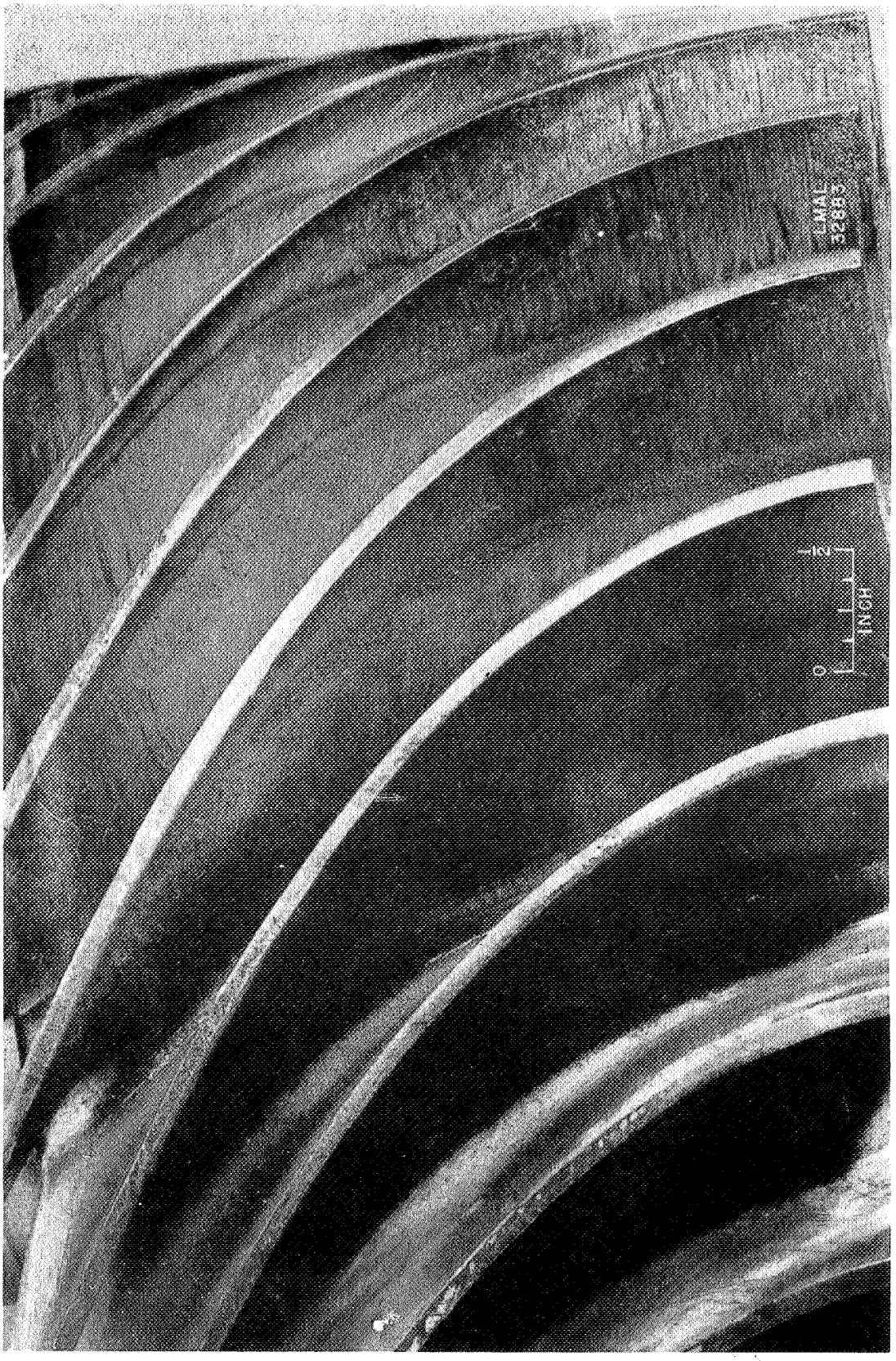


Figure 17. - Lampblack flow pattern on pressure side of blades of 4-inch, 24-blade inducer.

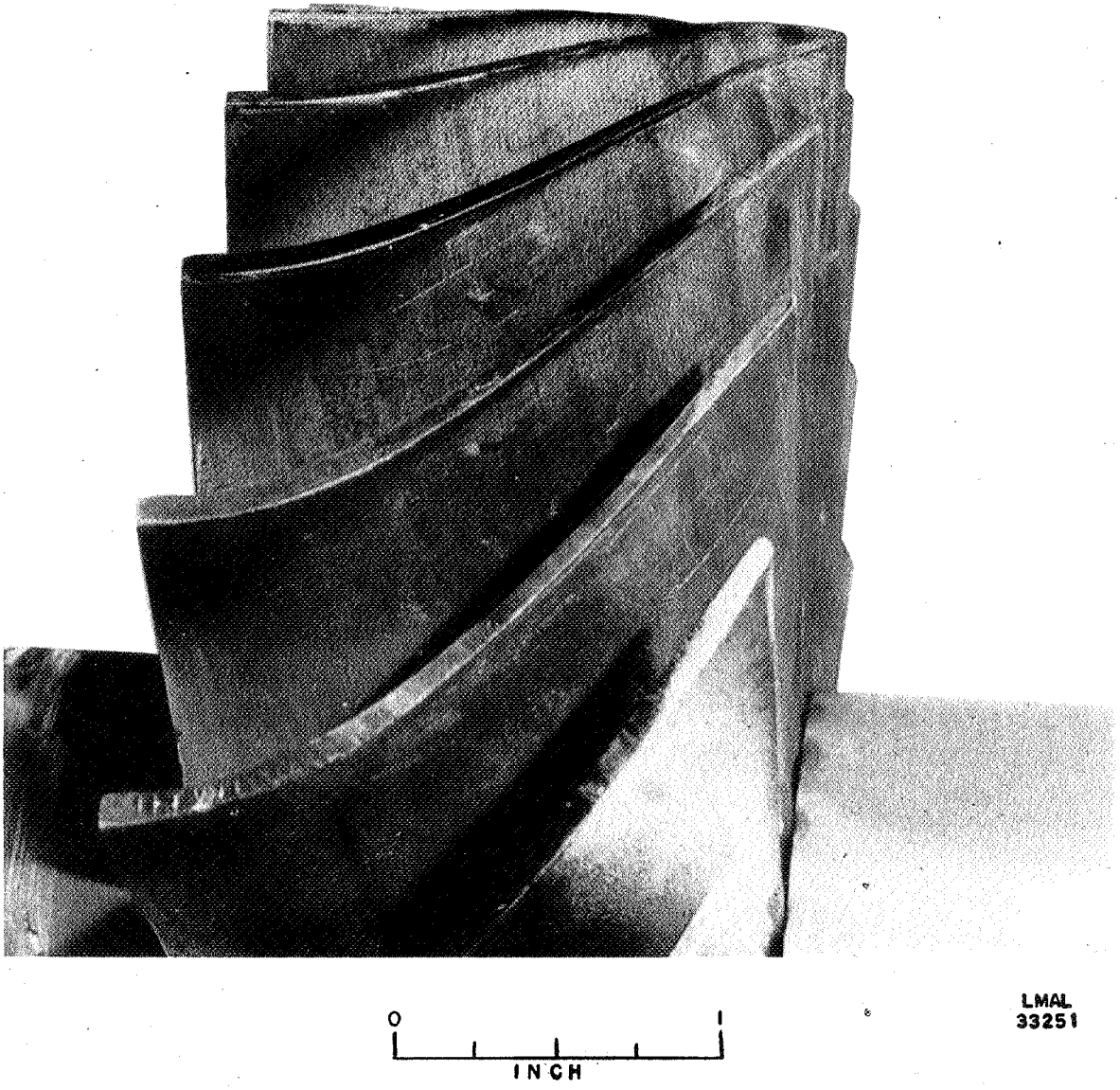


Figure 18. - Lampblack flow pattern on convex side of blades of 2-inch, 24-blade inducer.

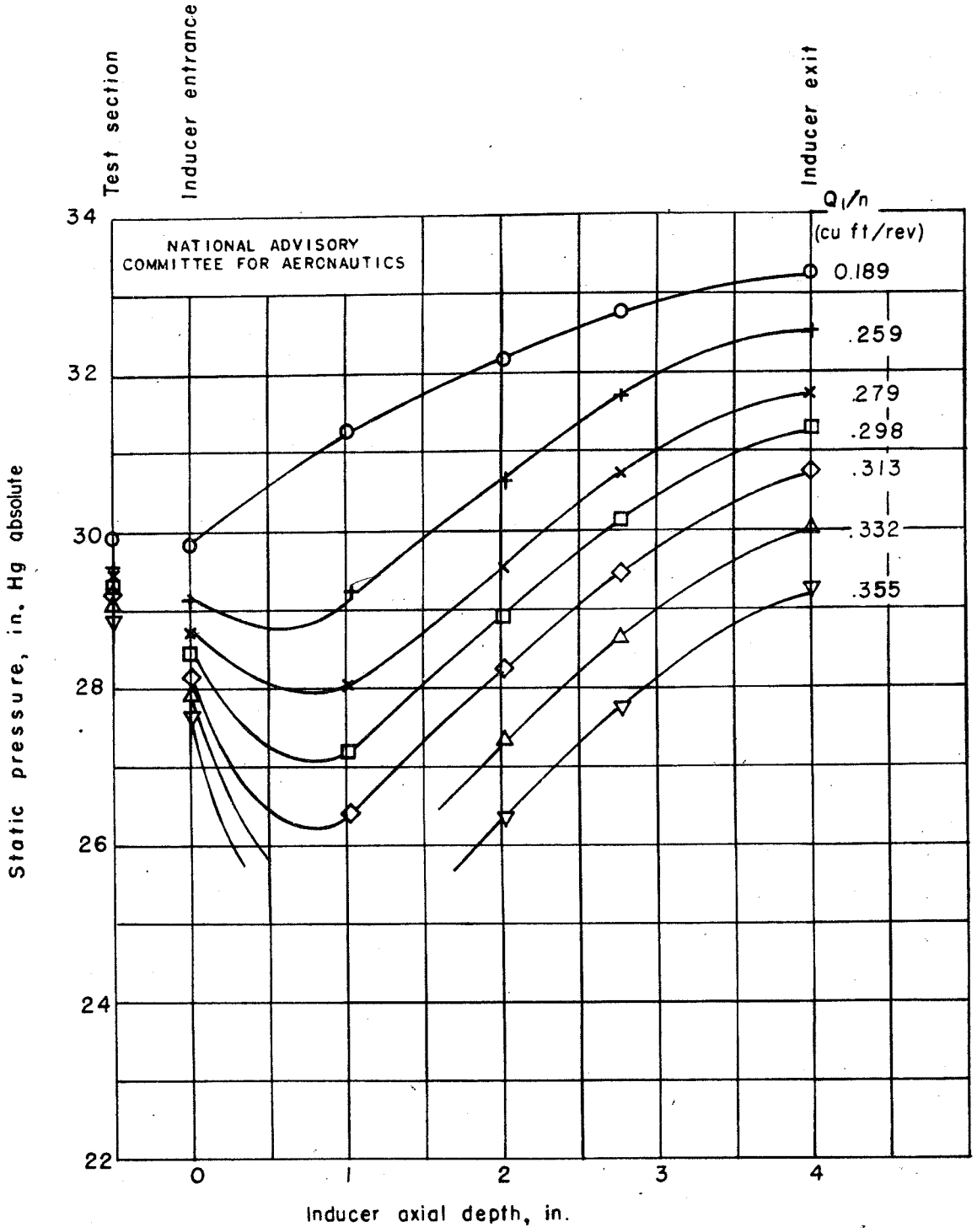


Figure 19.— Static pressure at wall of test section for 4-inch, 24-blade, rounded-edge inducer at equivalent tip speed of 800 feet per second.

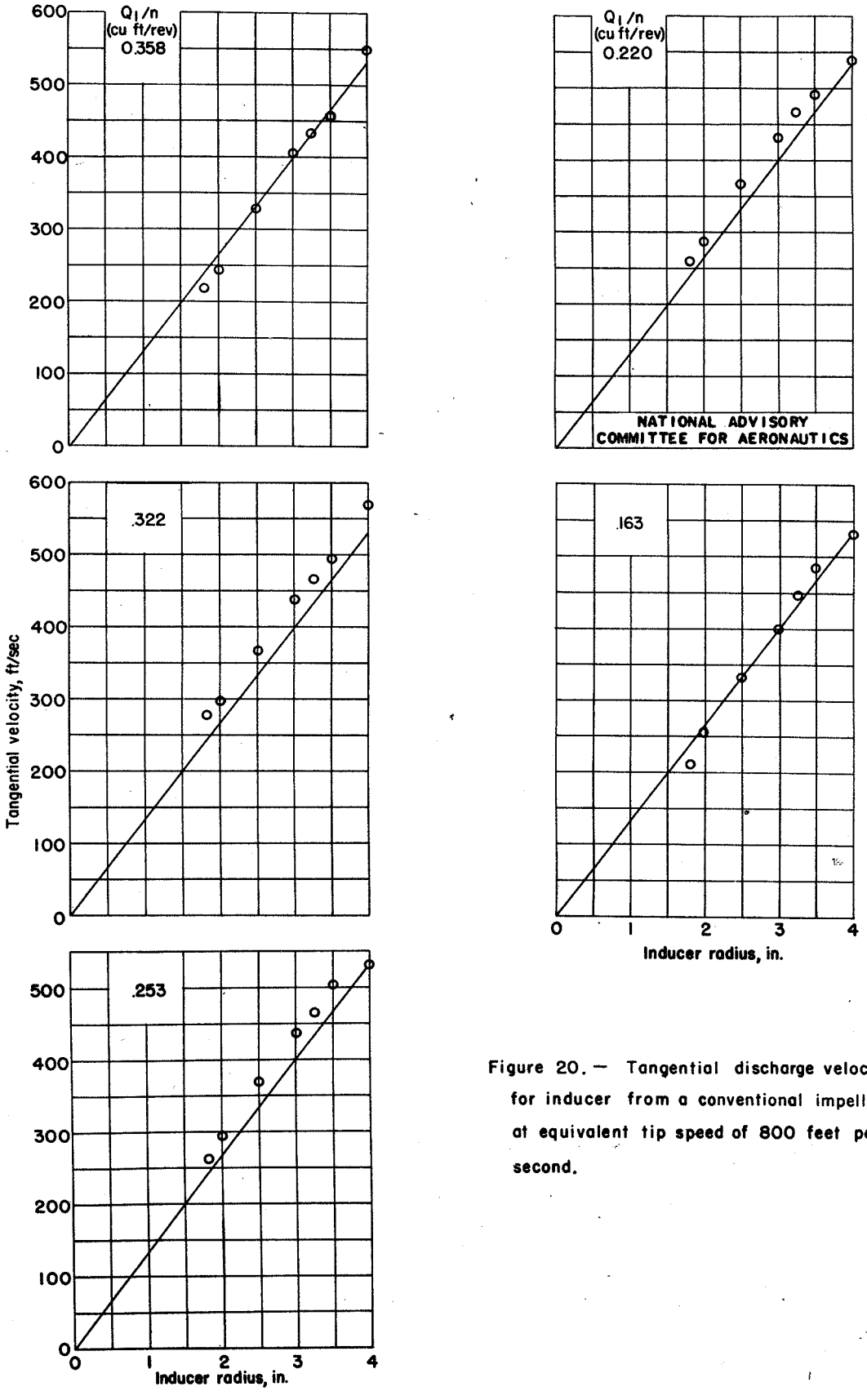


Figure 20. — Tangential discharge velocities for inducer from a conventional impeller at equivalent tip speed of 800 feet per second.

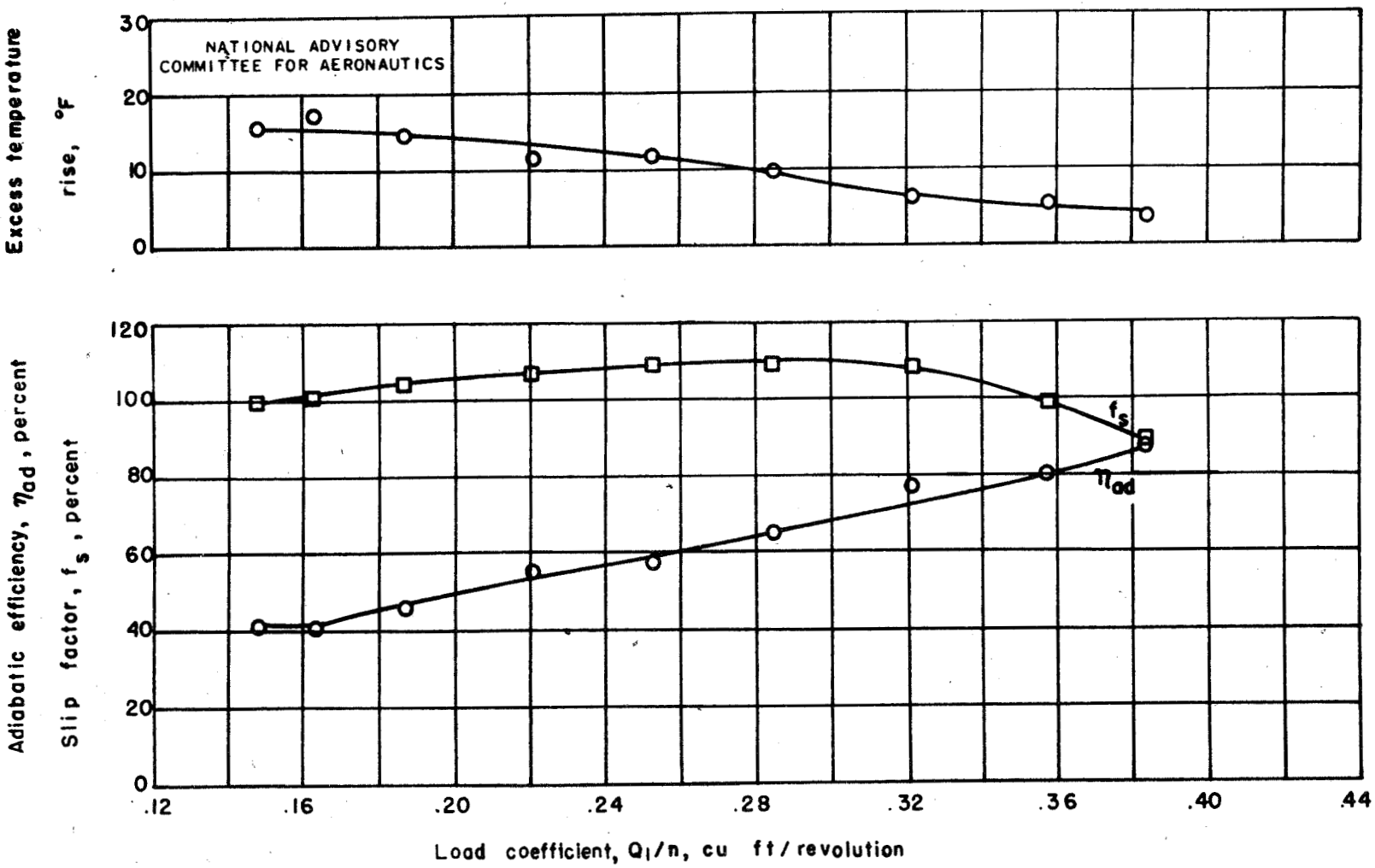


(a) Equivalent tip speed, 800 feet per second.

Figure 21.– Performance characteristics of inducer from a conventional impeller.

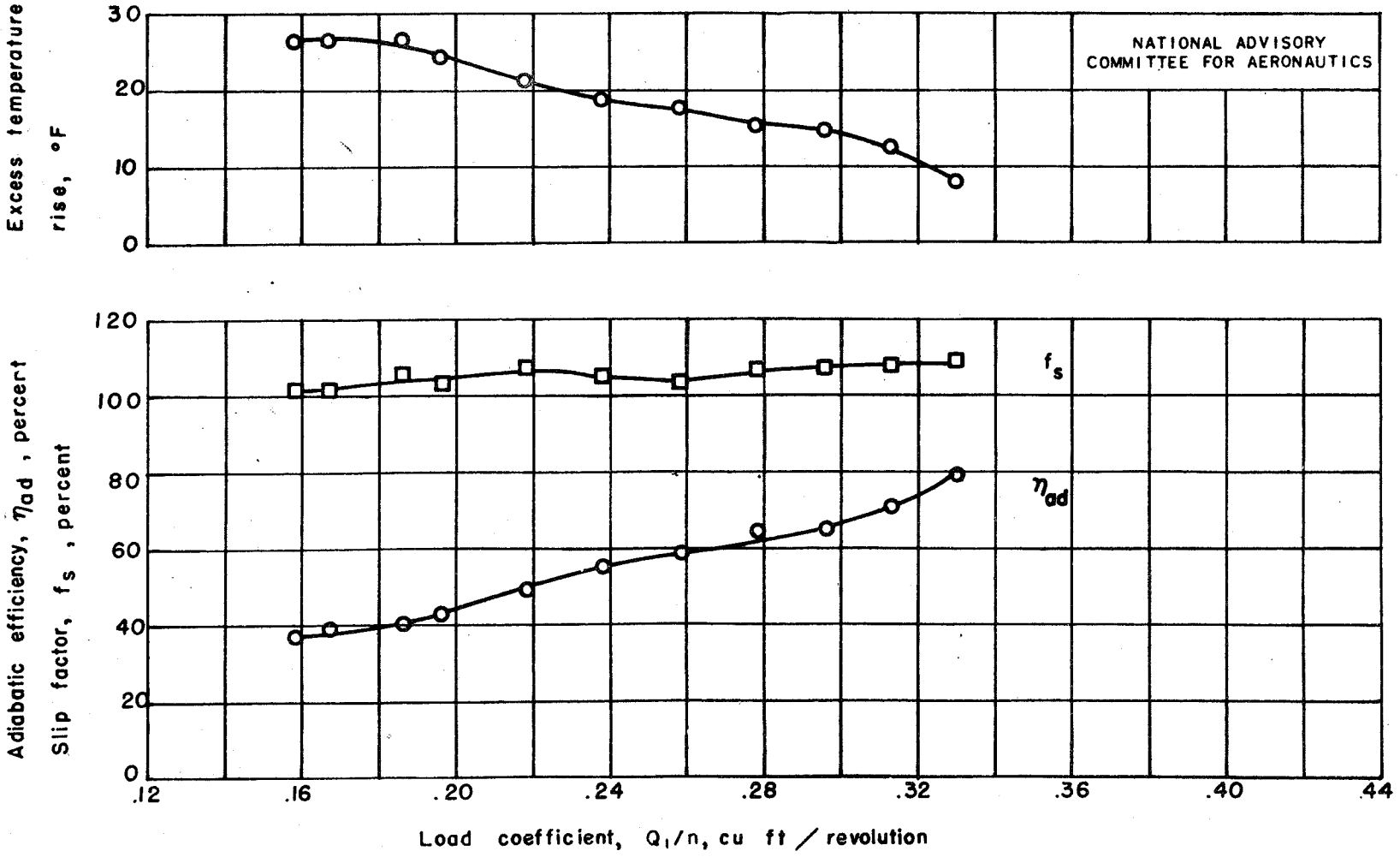


(b) Equivalent tip speed, 1000 feet per second.

Figure 21.– Continued.

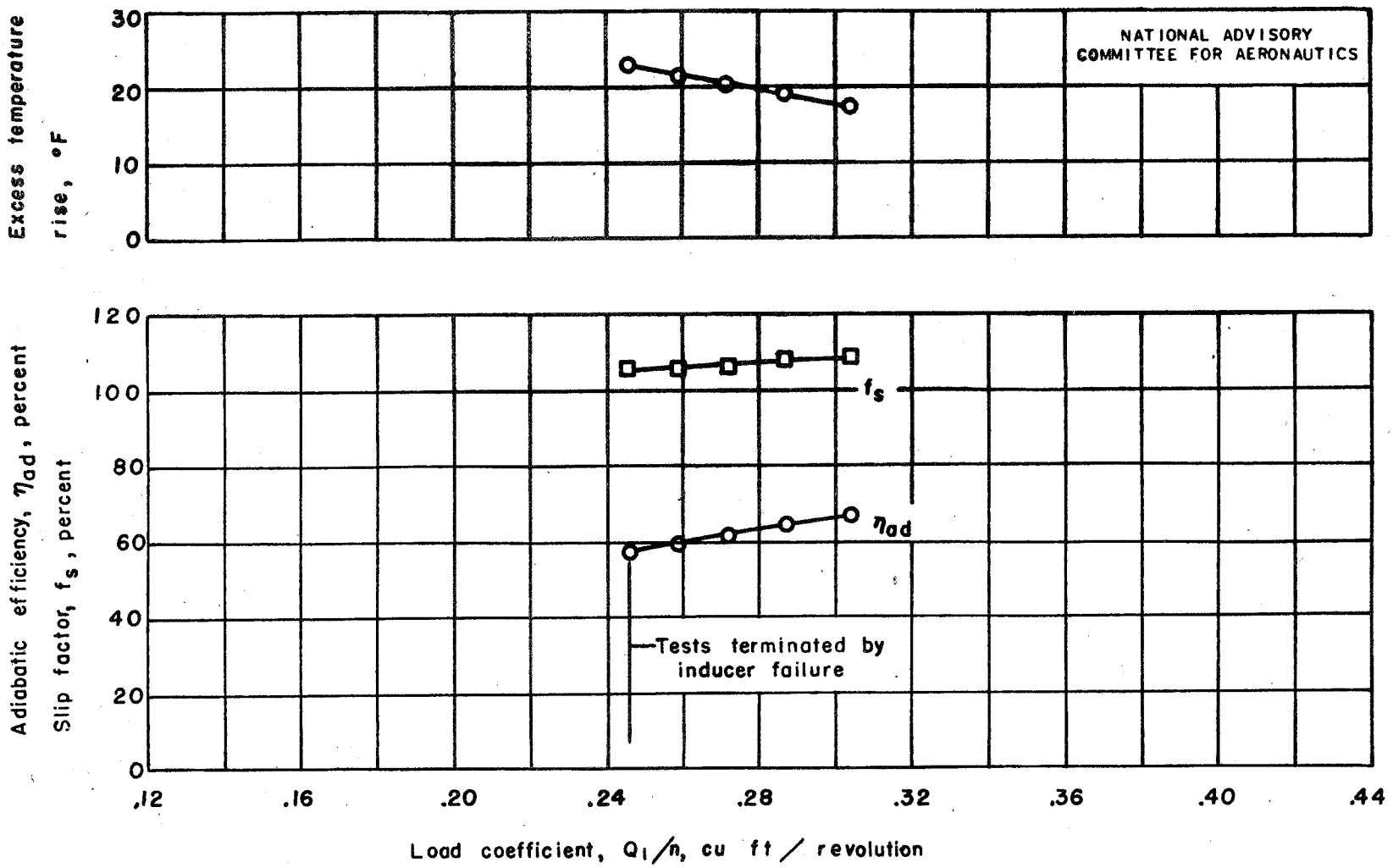


(c) Equivalent tip speed, 1100 feet per second.

Figure 21.– Concluded.